



Pergamon

Progress in Oceanography 41 (1998) 69–109

**Progress in
Oceanography**

Across-slope relations between the biological populations, the euphotic zone and the oxygen minimum layer off the coast of Oman during the southwest monsoon (August, 1994)

P.J. Herring*, M.J.R. Fasham, A.R. Weeks, J.C.P. Hemmings,
H.S.J. Roe, P.R. Pugh, S. Holley, N.A. Crisp, M.V. Angel

Southampton Oceanography Centre, Empress Dock, Southampton SO14 3ZH, UK

Abstract

An area some 120×70 km off the eastern coast of Oman (containing the UK JGOFS Arabesque station) was intensively studied over a 17 day period in August 1994, with the objective of determining the relationships between the biological populations, the oxygen minimum layer and the dynamic hydrography of the euphotic zone. The outer margin of the area was delimited by a rectangle of 15 full depth CTD casts and the hydrography was further defined by two Seasoar surveys within the box. Midwater trawls were used to sample the populations at three stations, oceanic, slope and shelf edge respectively. Day and night samples of macroplankton and micronekton were taken at each station to determine the extent of diel vertical migration and the effect of the hypoxic region on these migrations. Concurrent ADCP data were used to follow the migrations and spatial changes in real time. Despite the limited area studied the patterns of upwelling and their temporal and spatial changes were complex. Coastal upwelling was observed directly only at the southwestern edge of the area during both Seasoar surveys. Persian Gulf Water was a consistent but spatially discrete feature of the region at depths of 200–300 m. Arabian Sea Surface Water was present at the eastern margin of the first survey. Between these two water masses was a large area with small horizontal gradients and variable silicate and chlorophyll levels. Satellite data suggest that this water may have been advected as a filament from a more northerly coastal source. Very marked changes took place in the hydrography and in the phytoplankton composition and abundance at the reference station at 19°N 59°E over the 16 day period between visits. The highest biomass of plankton and micronekton (expressed as wet volume or as carbon) occurred in the upper 100 m, closely correlated with the relatively high oxygen levels at these depths. Gelatinous animals predominated in these layers, with additional swarms of swimming crabs. Quite large popu-

* Corresponding author.

lations of myctophid and photichthyid fishes and of decapod crustaceans were present below the oxycline by day. Most of these migrated into the surface layers at night, leaving minimal biomass behind, with the result that the ADCP backscatter data from beneath the oxycline at night were often below instrument resolution. Daytime ADCP data, on the other hand, showed multiple fine layering, some of which correlated with salinity differences. At the base of the oxygen minimum layer there was a large increase in biomass, marking the presence of a more typical bathypelagic fauna. © 1998 Elsevier Science Ltd. All rights reserved.

Contents

1. Introduction	70
2. Sampling area and methods	73
2.1. Sampling positions	73
2.2. Hydrographic and bioacoustic measurements	74
2.3. Net sampling	75
3. Results	76
3.1. General hydrography	76
3.1.1. CTD data	76
3.2. Seasoar surveys	80
3.2.1. Seasoar survey 1	80
3.2.2. Seasoar survey 2	83
3.3. Phytoplankton composition	87
3.3.1. Spatial variability during the first seasoar survey	87
3.3.2. Temporal variability	87
3.4. Acoustic backscatter	89
3.4.1. Diel vertical migration	89
3.4.2. Multiple layering	92
3.4.3. Relationship with seasoar data	93
3.5. Biomass data	93
3.5.1. Mesozooplankton (LHPR samples)	93
3.5.2. Macrozooplankton (RMT1 samples)	95
3.5.3. Micronekton (RMT8 samples)	95
4. Discussion	100
5. Acknowledgements	105
6. References	106

1. Introduction

The closed northern margin of the western Indian Ocean, combined with the seasonally reversed wind-forcing arising from the Southwest and Northeast Monsoons, results in a unique oceanographic region with dramatic seasonal changes in circulation, mixed layer depth, and biology. It is most clearly characterized by the presence of a permanent hypoxic layer (Wyrski, 1971, 1973; Qasim, 1982; Swallow, 1984). This layer extends for almost 1 km below the very steep oxycline which occurs at a depth of about 100 m; it is present over much of the northwestern Indian

Ocean, diminishing in intensity westward within the Gulf of Oman and southward of about 10°N. Swallow (1984) proposed that the layer is maintained by input of water at intermediate depths (from the southern Indian Ocean, from the Red Sea and from the Persian Gulf) which is already relatively low in oxygen. The layer is not a sluggish water mass: tracer measurements using Freon-11 indicate that it has a residence time of only about 10 yr (Olson et al., 1993). These authors developed Swallow's (1984) proposal by using a box model to calculate an oxygen budget for the region, in the context of different potential generative mechanisms. They concluded that the low oxygen inflow, when combined with realistic estimates of in situ oxygen demand, which arises from the decomposition below the oxycline of the substantial "new" production, results in the very thick low-oxygen layer, limited at its base by the intrusion of North Indian Deep Water. It was not necessary to invoke an intense oxygen sink, generated by a very large input of organic matter from the euphotic zone, such as occurs off the coast of Peru (Packard et al., 1983). These calculations were further refined by Warren (1994) who showed that the major input from the south (with a sea-surface source at latitudes 40°–50° S) had a sufficient travel time (ca 30 yr) for its oxygen concentration to be reduced to the level observed in the South Arabian Sea. The circulation and upwelling patterns in the Arabian Sea and Somali Current region are complex, with the intense winds of the Findlater Jet producing wind curl effects resulting in upward Ekman pumping and consequent upwelling occurring up to several hundred km offshore (Bruce, 1974; Smith and Bottero, 1977; Swallow, 1984; Bauer et al., 1991). At the same time the Southwest Monsoon creates the classic conditions for coastal upwelling, with offshore surface transport and upwelling from depths of about 150 m (Smith and Bottero, 1977; Smith et al., 1991; Bauer et al., 1991; Currie, 1992; GLOBEC, 1993; Shetye et al., 1994; R. L. Smith, 1995).

The very high seasonal productivity resulting from the upwelling events, induced by the strong winds of the Southwest Monsoon, contributes to the elevated subthermocline regional oxygen demand and hence to the seasonal maintenance of the low oxygen water mass. Primary production in the surface mixed layer is not affected directly by the low oxygen layer, but the overall biological structure of the populations in both the mixed layer and the low oxygen layer is affected by the ability of particular species to endure the oxygen deprivation of life below the oxycline, i.e. within the mesopelagic realm. Most studies of such a situation have hitherto been focused on the Eastern Tropical Pacific Ocean (Longhurst, 1967; Judkins, 1980; Wishner et al., 1995, and references therein). The more limited studies of the Arabian Sea in this respect have shown that the zooplankton in the Arabian Sea appears to be restricted mainly to waters above the oxycline (Vinogradov and Voronina, 1962; Vinogradov, 1970; Van Couwelaar, 1997) with some enhancement at the base of the oxygen minimum layer (Koppelman and Weikert, 1997). Diel vertical migration (from daytime upper mesopelagic depths into the surface layers at night) provides one physiological compromise. The abundance and feeding effects (both predatory and grazing) of species carrying out such migrations will modify the structure of the populations within the surface mixed layer. The occurrence of scattering layers descending daily from the mixed layer to 200–300 m indicates the extent of this

migration. They are probably primarily caused by myctophid fishes, whose local densities can achieve commercial levels (Gjosaeter, 1981, 1984) and whose feeding ecology will have a major impact on the consumers of the primary production (Dalpadado and Gjosaeter, 1988; Kinzer et al., 1993).

Much of the considerable effort devoted over the last 40 years to the analysis of the biological and physical environment of the region has focused on the circulation and the forcing effects of the seasonal upwelling and primary production, usually through extensive international surveys of the circulation, surface mixed layer and the biogeochemical fluxes (IIOE (Zeitschel and Gerlach, 1973), WOCE, (WOCE, 1992, 1993), JGOFS (Smith et al., 1991; Smith, 1984; Baars, 1994) and GLOBEC (GLOBEC, 1993)). Less attention has been paid to the biology of the mesopelagic fauna, with the result that even the qualitative faunal composition and its vertical distribution are still very poorly known (GLOBEC, 1993; Banse, 1994). Some quantitative surveys have been carried out with closing nets as part of the JGOFS Netherlands Indian Ocean Programme (NIOP) further south (from the Somali Basin to the Gulf of Aden; Schalk and Van Couwelaar, in Baars, 1994; Van Couwelaar, 1997) and there are recent data on myctophid distributions from oblique, open, Isaacs-Kidd Midwater Trawl tows to the north and east (Kinzer et al., 1993), as well as those from the exploratory studies with open commercial trawls in the Gulf of Oman (Gjosaeter, 1981, 1984). In addition Koppelman and Weikert (1997) have examined the quantitative vertical distribution of mesozooplankton throughout the water column.

The overall objective of the scientific programme of Discovery Cruise 209 was to carry out an intensive quantitative analysis of the vertical distribution of the macroplankton and micronekton in relation to the low oxygen water, at oceanic, slope and shelf locations during the Southwest Monsoon. A sampling area off the eastern coast of Oman, just to the east of Ras Madraka, was chosen to provide access to all three depth regimes, within an area small enough for us to be able to characterise the associated mixed layer events in detail at the same time (Fig. 1). The area lies between sections IV and V of the Discovery 1963 offshore transects (Currie, 1992), and very close to Charles Darwin cruise 26 section D (Elliott and Savidge, 1990) sampled at a similar time of year (19–26 August 1987). This paper describes the main results and conclusions of this programme.

The oceanic station at 19°N 59°E was designated as the UK “Arabesque” reference station within the JGOFS Indian Ocean programme. This has allowed subsequent cruises to carry out longer term monitoring of the temporal changes in the biogeochemistry at the site (e.g. Mantoura, 1995).

2. Sampling area and methods

2.1. Sampling positions

The entire sampling programme was contained within a box 120 km × 70 km, extending from deep water in the Owen basin up to the shelf edge, and occupied

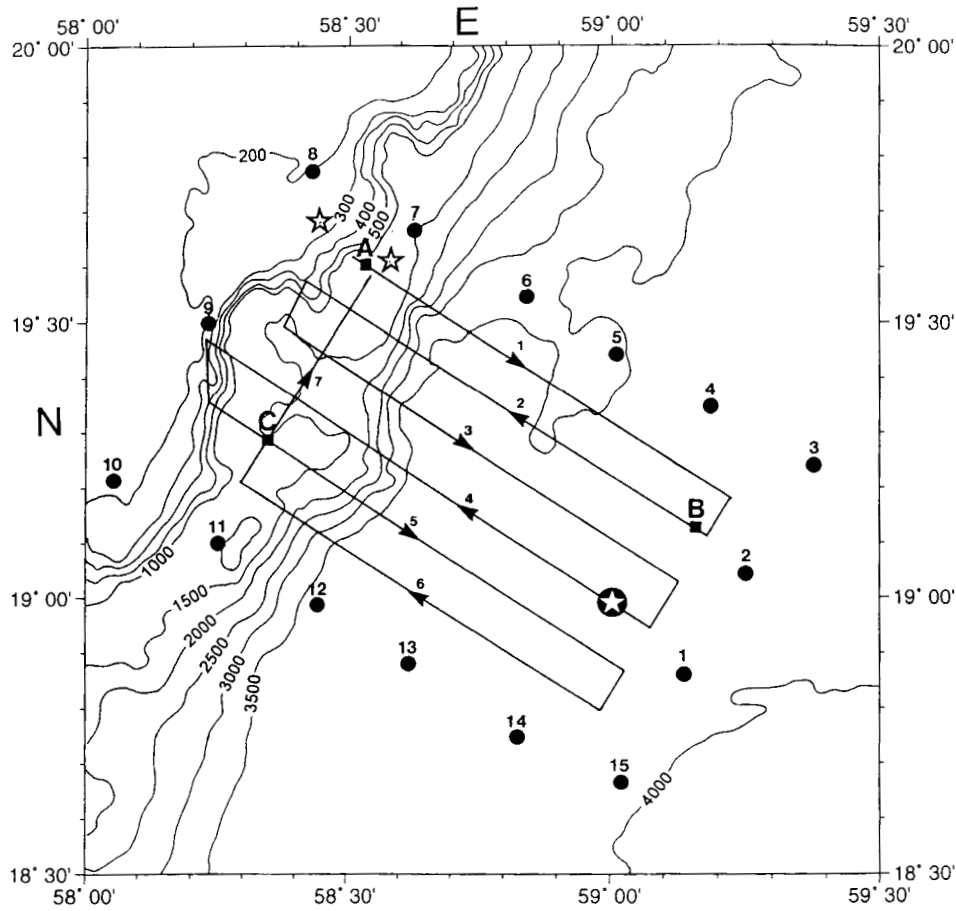


Fig. 1. Topographic chart of survey area, showing the positions of CTD stations 1–15 and the track plot of Seasoar survey 1 (legs 1–7). Also shown are the Arabesque reference station (circled star), the slope and shelf trawling positions (stars), and the positions of the phytoplankton samples (A,B,C). Depths are in m.

from August 4–21, 1994. The margins of the box were delimited by a series of 15 CTD casts to the bottom (Fig. 1, Table 1), and two Seasoar surveys were carried out within the box (August 10–12 and 16–18). In addition, the Arabesque reference station at 19°N 59°E was occupied twice (August 5: *Discovery* Stn 12664 and Aug 21: *Discovery* Stn 12670), for full depth CTD profiles and for tows of the Longhurst-Hardy Plankton Recorder (LHPR) on each occasion. The shelf, slope and oceanic trawling stations (Stn 12668: 19° 36'N 58° 25'E, Stn 12667: 19° 31'N 58° 34'E and the Arabesque station, Stn 12664), also lie within the CTD survey box (Fig. 1).

Table 1
CTD station positions in the box survey shown in Fig. 1

CTD Box No.	Date	Latitude (°N)	Longitude (°E)	Depth (m)
1	6/8/94	18 50.3	59 08.3	3436
2	6/8/94	19 01.3	59 15.3	3395
3	6/8/94	19 13.1	59 23.2	3384
4	7/8/94	19 19.7	59 11.8	3263
5	7/8/94	19 26.2	59 00.6	2779
6	7/8/94	19 32.6	58 49.2	2896
7	7/8/94	19 39.5	58 38.1	1078
8	7/8/94	19 46.7	58 25.6	91
9	7/8/94	19 30.1	58 14.5	113
10	8/8/94	19 12.1	58 03.0	78
11	8/8/94	19 05.3	58 14.4	922
12	8/8/94	18 58.6	58 25.6	3142
13	8/8/94	18 51.8	58 37.0	3266
14	8/8/94	18 45.1	58 48.4	3105
15	9/8/94	18 38.4	59 00.1	3462

2.2. Hydrographic and bioacoustic measurements

CTD casts were made with a Neil Brown Mk IIIB CTD and Beckman polarographic dissolved oxygen sensor, on a 24 bottle General Oceanics multisampler with 10l FSI or E & G water bottles. The package included a Sea Tech 100 cm transmissometer and a Chelsea instruments Mk II fluorometer. Salinity, oxygen and chlorophyll were determined from the water bottles (according to World Ocean Circulation Experiment protocols) and were used to calibrate the CTD and fluorometer. Nutrient samples were taken for nitrate (and nitrite), phosphate and silicate determination. Phytoplankton samples were taken from bottles in the upper 100 m of specific casts.

Seasoar is a towed undulating sensor package which typically carried a Neil Brown Mk IIIB CTD, Chelsea Instruments Mk II fluorometer and 2π PAR, irradiance and radiance sensors (e.g. Allen et al., 1994). At a speed of 8 knots the undulation is normally between the surface and ca 400 m, with a spatial resolution at the surface of ca 4 km. Data are averaged vertically over 4 dbar (\cong 4 m) and horizontally over 4 km (for details of data processing and calibration see Allen et al., 1994). For the first survey the vehicle carried a 2π PAR sensor (Plymouth Marine Laboratory). For the second it carried Satlantic irradiance and radiance sensors; the data from these are described by Weeks et al. (1997). Seasoar's operational depth capability for the second survey was about 250 m. During the Seasoar surveys surface samples of salinity and chlorophyll were taken from the ship's non-toxic seawater supply every 2 hr, with the sample timed to correspond to the vehicle's approach to the surface. These samples were used to calibrate the Seasoar salinity (using a Guildline S400 salinometer) and fluorescence data (Turner Designs fluorometer, regularly calibrated against a pure chlorophyll *a* standard). Data were calibrated to better than 0.01 (salinity), 0.005°C (temperature) and 0.1% (pressure). The Seasoar oxygen sensor

data were not used because of hysteresis difficulties. In addition to the 2 hourly surface sampling, surface fluorescence data were logged throughout the cruise, using a laboratory Turner Designs model 10-000R fluorometer fitted with a flow-through cell. These instruments, plus a surface thermosalinograph and an in-line autoanalyser for surface phosphate and silicate (modified Technicon AA 11 system), were fed from the ship's de-bubbled non-toxic seawater supply, from which phytoplankton samples were also taken at intervals throughout the cruise. The autoanalyser water was filtered through a continuous filter block containing a pre-rinsed (10% HCl) 0.45 μm Millex filter.

Current vectors and acoustic backscatter data were obtained with a hull-mounted 150 kHz Acoustic Doppler Current Profiler (ADCP; RD Instruments). The use of the ADCP to provide a range of biological information is now well established (Flagg and Smith, 1989; Plueddemann and Pinkel, 1989; Roe et al., 1996; Weeks et al., 1995). Absolute acoustic backscatter is calculated either by using the manufacturers' equation for Mean Volume Backscatter (MVBS) (RD Instruments, 1990)—which assumes a constant value for α (the sound absorption coefficient)—or, when concurrent Seasoar temperature and salinity data were available, using the method described in Roe et al. (1995, 1996) which corrects for variations in α . The accuracy of the resultant MVBS has been estimated by Griffiths and Diaz (1996) by comparing the data with the 200 kHz channel of a Simrad EK 500 sounder. They concluded that the ADCP can give estimates of MVBS at the 95% confidence level to better than ± 1.5 dB — sufficient accuracy to couple the biology and physics on the scales considered here. The ADCP data are averaged over 10 min with a bin depth of 4 m (corresponding roughly to the Seasoar averaging). Further details of the ADCP and Seasoar data processing, and an atlas of concurrent hydrography and acoustic backscatter throughout the cruise, are given in Roe et al. (1995).

2.3. Net sampling

Bathymetric profiles of the biological populations at the oceanic, slope and shelf stations were made through a series of horizontal tows with a multiple rectangular midwater trawl system (RMT1 + 8M). This consists of three pairs of nets fished consecutively, each pair comprising a net with a 1 m² mouth area and 0.33 mm mesh (RMT1, for macrozooplankton) and a net with an 8 m² mouth area and 4.5 mm mesh (RMT8, for micronekton) (Roe and Shale, 1979; Roe et al., 1980). The upper 200 m of the water column was divided into four 50 m bands and greater depths into 100 m bands. All tows were of 1 hr duration. A day and a night series of samples was taken at each position to investigate the extent of diel vertical migration. "Night" samples were defined as those taken from one hour after sunset to one hour before sunrise; "day" hauls were from one hour after sunrise to one hour before sunset. Below 1000 m no distinction was made. Day and night samples were taken on the shelf to 170 m. At the slope station day and night samples were taken to 400 m and an additional day sample from 400–500 m. At the oceanic station day and night samples were taken to 900 m, with an additional day sample from 900–1000 m. Three 200 m samples were taken between 1200m and 1800m, with the trawl times extending

across the day/night boundary. RMT8 samples were obtained from all depths fished, but the severe sea conditions damaged several of the RMT1 nets and some of these samples were therefore not collected.

Two parameters have been used to quantify the biomass of the catches: (1) normalised displacement volumes and (2) carbon content, estimated from the displacement volumes. Displacement volume is a non-destructive measure of biomass and replicate measurements indicate that the range of error is 5–10%. Errors also stem, however, from the inclusion of interstitial water, but it is destructive to the specimens if attempts are made to overcome this. The preserved RMT8 samples were first volumed in toto, then sorted to the main groups and the volumes of each group measured separately. Copepods were excluded from this analysis because they are not sampled quantitatively by the RMT8 nets (Hubold et al., 1988). RMT1 samples were volumed without sorting. Carbon was estimated from the RMT8 displacement volumes using the amended formula of Wiebe (1988) for non-gelatinous organisms, and, for gelatinous organisms, a value calculated from the data from Larson (1986) (see Pugh et al., 1997), which indicates that 1 ml displacement volume is equivalent to 3.649 mg carbon. Gelatinous taxa were taken to be siphonophores, medusae and tunicates, with the last playing a very minor role. Non-gelatinous organisms included fish, crustaceans, chaetognaths and any other groups remaining from the sorted catches. Ikeda (1974) reported lower carbon values for tropical zooplankton than for temperate ones, with particular emphasis on copepods. We have not converted our zooplankton (RMT1) data to carbon, only our nekton (RMT8) data (see Results) and consider Wiebe (1988) formula is appropriate for this, even though it is derived largely from temperate Atlantic material.

Two oblique tows for mesozooplankton were made at the Arabesque station with the Longhurst-Hardy plankton recorder (LHPR) towed at 4B5 kt (mesh size 200 μ m; 2 min samples). On each occasion the LHPR sampled from the surface to a depth of 250 m, and back to the surface.

3. Results

3.1. General hydrography

3.1.1. CTD data

The water mass characteristics of this area have been described by Currie (1992) in terms of salinity minima and maxima. Figure 2a shows the θ -S curves for four CTD stations (#16, #18, #21, #22 correspond to positions 11, 13, 14, and 15 respectively in Fig. 1) from the southernmost transect (Table 1). Contoured sections of salinity, density and oxygen for the northern and southern CTD stations are shown in Fig. 3a–c (3–8 and 10–15, respectively, in Fig. 1). The most prominent feature is the high salinity Persian Gulf Water (PGW) at 100–350 m. This flows southwest along the Omani coast between σ_t surfaces of 26.0 and 27.0 (Currie, 1992), whereas the main core of the PGW spreads further east and along the west coast of India

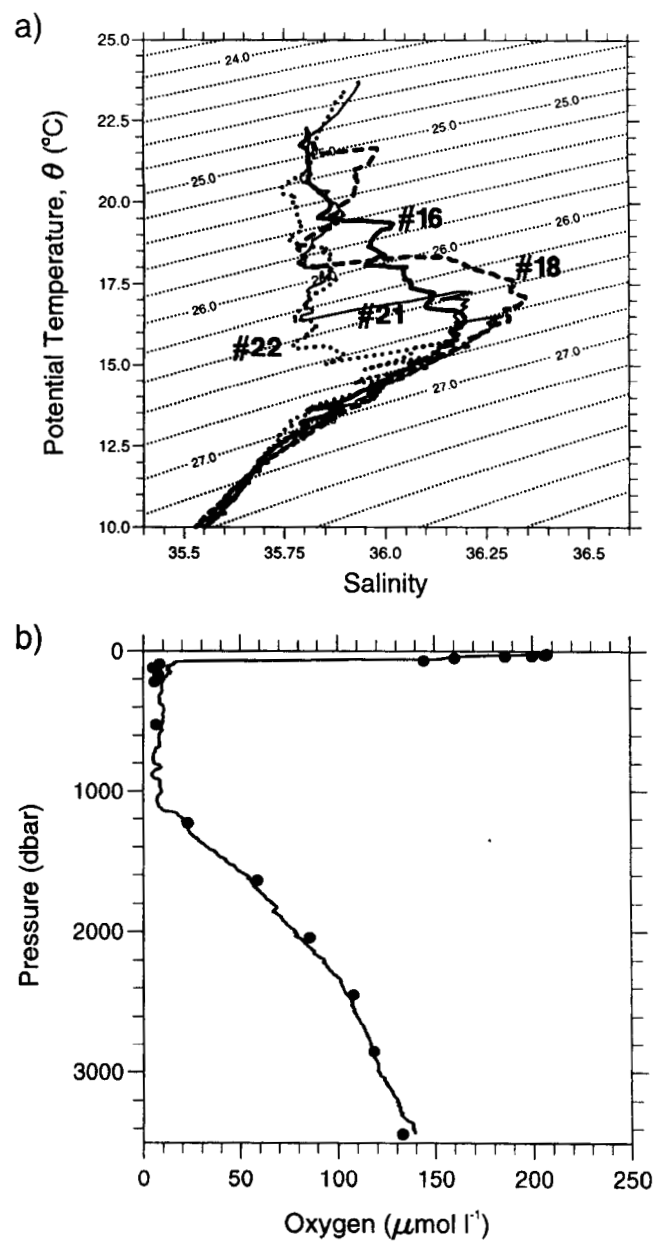


Fig. 2. (a) θ -S curves from selected CTD profiles on the southern CTD transect (at positions 11,13,14 and 15 in Fig. 1 and Table 1), (b) Calibrated CTD oxygen sensor profile and bottle data at the Arabesque station on 5 August.

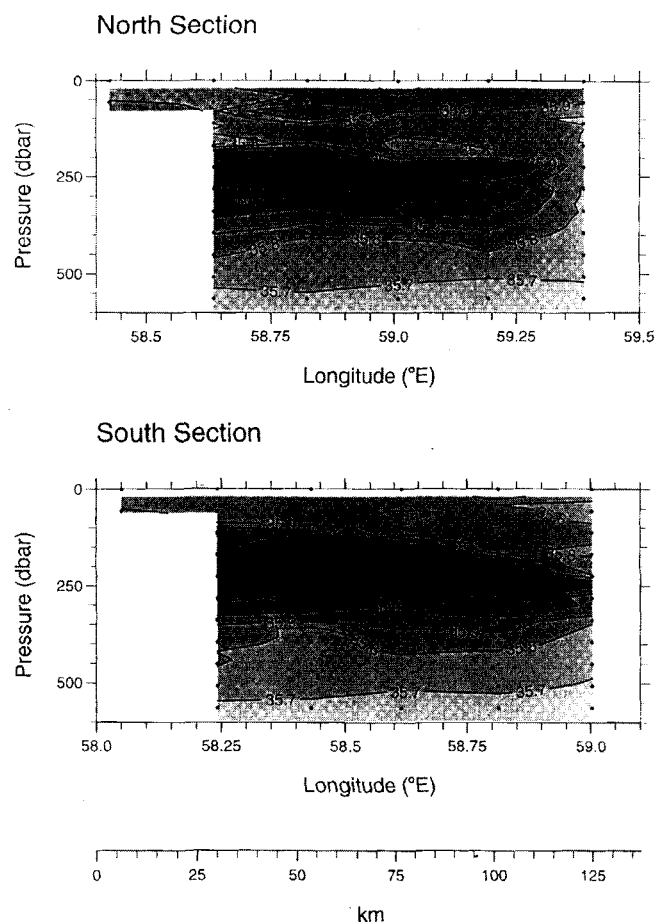
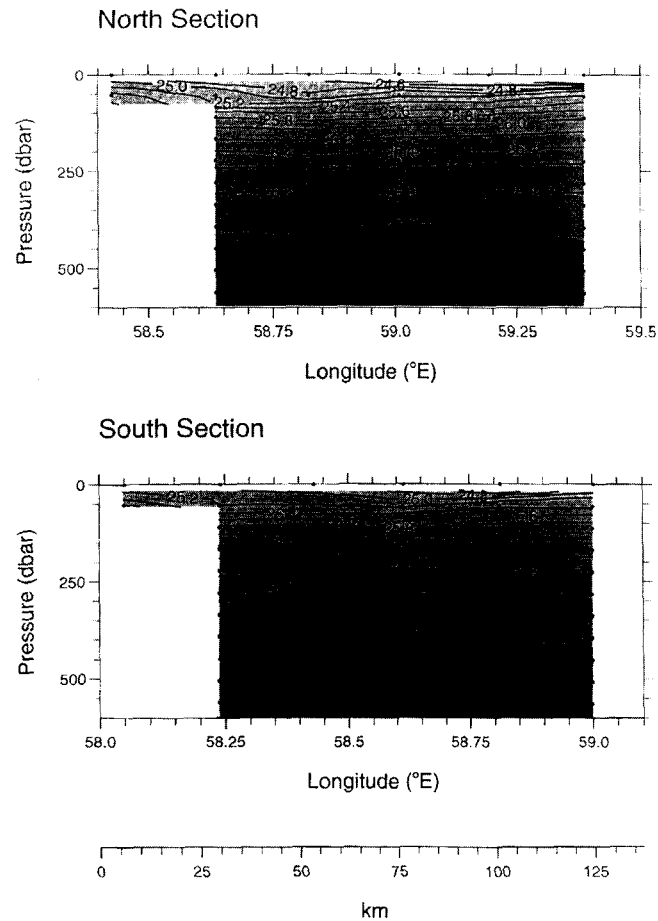


Fig. 3a. (a) Northern and southern east-west CTD sections (3–8 and 15–10 respectively in Fig. 1: 0–600 m) showing contours of (a) salinity (psu), (b) σ_{θ} (kg m^{-3}), and (c) oxygen ($\mu\text{mol l}^{-1}$) (following pages). CTD stations are indicated by dotted lines. In this and all subsequent figures of contoured sections the shelf edge is to the left.

(Premchad et al., 1986). Above the PGW there is generally a salinity minimum with values in the range 35.75–35.86 and above this lies more saline near-surface water.

The concentration of oxygen declines very rapidly below the euphotic zone and levels remain low until about 1100 m (Fig. 2b) (cf. data for the adjacent NIOP Stn 485 in Theberge et al., 1997). Variations in the depth of the oxycline are closely correlated with variations in the depth of the isopycnals (Fig. 4). Oxygen concentrations within the oxygen minimum layer are not spatially uniform in the surveyed area, but show an increase from west to east (Fig. 3c), in the opposite direction to the large scale trend in the northern Indian Ocean (Wyrki, 1971). The two lowest recorded bottle oxygen values were 0 and $0.04 \mu\text{mol l}^{-1}$, with a precision at these levels of $\pm 0.02 \mu\text{mol l}^{-1}$.

Fig. 3. Continued: 3b, sigma- θ .

The Arabesque reference station was occupied twice on the cruise (5 and 21 August 1994). Over this period of 16 days the mixed layer temperatures increased by 1.5° (Fig. 5b), and the mixed layer deepened from 20 m to 50 m (Fig. 5a). This deepening may have been caused partly by the high winds between 16 and 20 August (Fig. 6), but advective effects cannot be ruled out. On 5 August the chlorophyll *a* profile showed a subsurface maximum at a depth of 30 m, whereas on 21 August the maximum values were observed at the surface (Fig. 5d). Chlorophyll *a* values increased between the two occupations of the station, and this was reflected in a reduction in surface nitrate values (Fig. 5c). However, on neither occasion were the nitrate or silicate levels potentially limiting for phytoplankton growth.

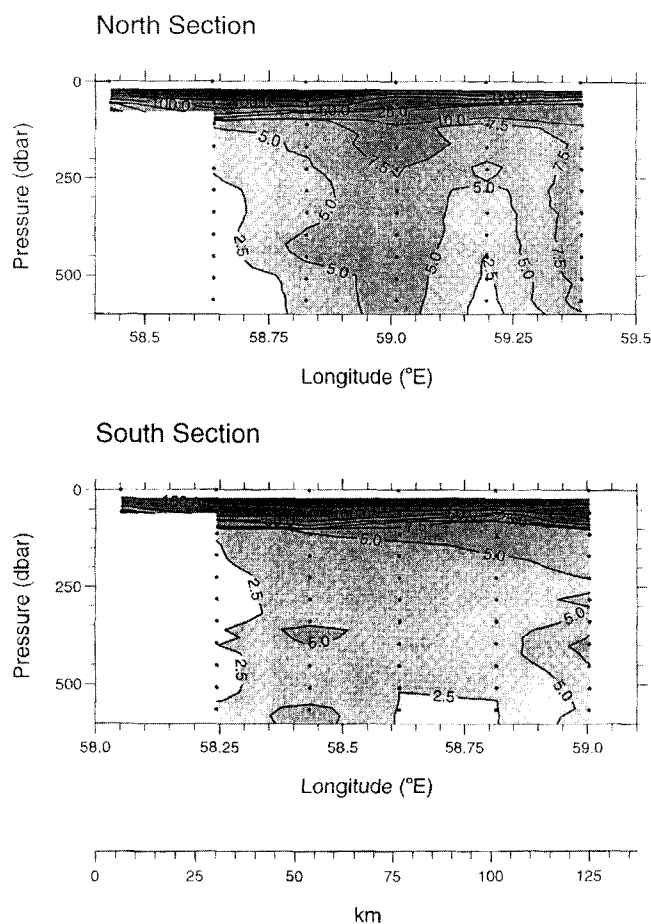


Fig. 3. Continued: 3c, oxygen.

3.2. Seasoar surveys

3.2.1. Seasoar survey 1

The first Seasoar survey was carried out between 10 and 12 August and the track plot is shown in Fig. 1. Most of the survey was in water deeper than 500 m but sections 4 and 5 extended up to the lower slope (300–400 m). During the survey the surface sea water was sampled from the non-toxic seawater supply with the thermosalinograph, fluorometer and in-line nutrient autoanalyser (see Methods). These data were contoured to give plots of surface temperature, salinity, chlorophyll *a* fluorescence and silicate concentrations. Technical problems rendered the surface nitrate and phosphate data unusable. The temperature, salinity and silicate data identify three surface features within the area surveyed (Fig. 7). At the western end of legs 4 and 5 there was a region with temperatures $< 21^{\circ}\text{C}$, low salinity and silicate

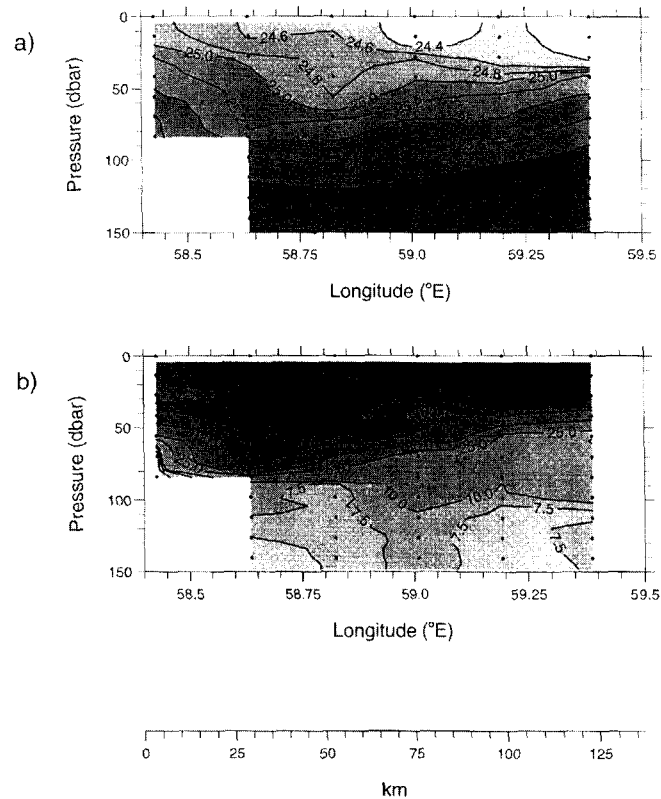


Fig. 4. Northern CTD (3–8) section (0–150 m) showing contours of (a) sigma- θ (kg m^{-3}), (b) oxygen ($\mu\text{mol l}^{-1}$).

as high as $14 \mu\text{mol l}^{-1}$. The association of low temperature and high nutrients implies that this was recently upwelled water. In the northeast was a small area with high temperatures and salinity (> 36) and low silicate which was sampled at the extreme eastern end of legs 1–3. The high salinity identifies this water as North Arabian Sea surface water (Currie, 1992). Between these two water types, and separated from them by strong frontal features, was a large area with small horizontal gradients in temperature and salinity but very variable chlorophyll and silicate concentrations.

All the long Seasoar sections showed similar features, so we show only one of them, leg 4, which passes through the Arabesque station (see Fig. 1). Colour contoured sections of temperature, salinity, stability (defined as $10^8 \cdot (d\rho/dz)/\rho$), chlorophyll *a* fluorescence, and ADCP absolute backscatter (dB) are shown in Fig. 8. The temperature plot shows clearly the upwelled water and the front to the east of it that is a normal feature of coastal upwelling (R. L. Smith, 1995) (Fig. 8a). The upwelled water had a density of $25.2\text{--}25.4\sigma_\theta$ and apparently came from a depth of about 80 m. The salinity of this water confirms that its origin is the low salinity water present between the high salinity surface water and the PGW (Fig. 2a).

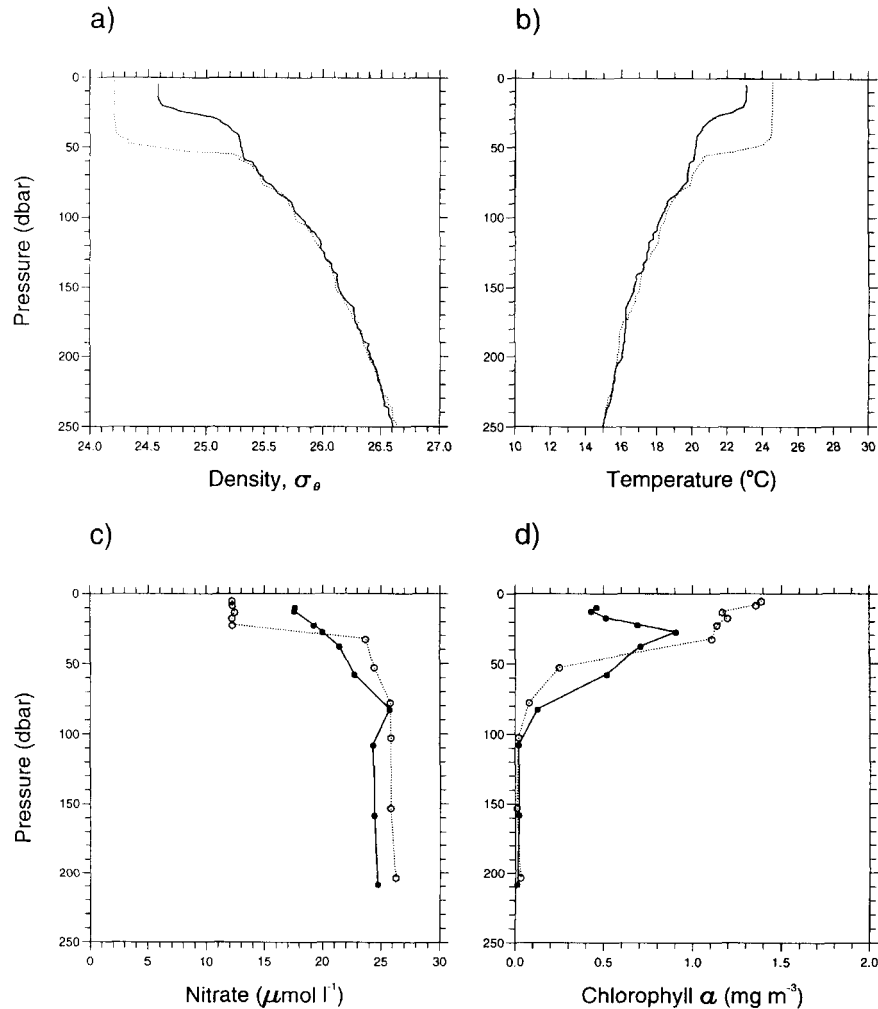


Fig. 5. Arabesque station profiles (0–250 m) on 5 August (solid lines) and 21 August (dotted lines). (a) density (kg m^{-3}), (b) temperature ($^{\circ}\text{C}$), (c) nitrate ($\mu\text{mol l}^{-1}$), and (d) phytoplankton chlorophyll *a* (mg m^{-3}).

The salinity section (Fig. 8b) is of particular interest in that it shows some of the fine structure of the PGW. The main core of this water is deeper than 150 m at σ_{θ} of 26.6 (Fig. 3a); this section shows the top of this core water as well as some small high salinity patches at lower densities ($\sigma_{\theta} = 25.2\text{--}25.6$). CTD profiles taken from *RRS Charles Darwin* in 1986 in the mouth of the Gulf of Oman show salinity maxima at such densities (Currie, 1992). The Seasoar data show that these shallow patches are only ~ 10 km wide and would be likely to be missed by a widely spaced CTD survey.

The chlorophyll *a* fluorescence section gives more data on the high chlorophyll *a* patch to the east of the upwelling front (Fig. 8d). It is bounded below by a shallow

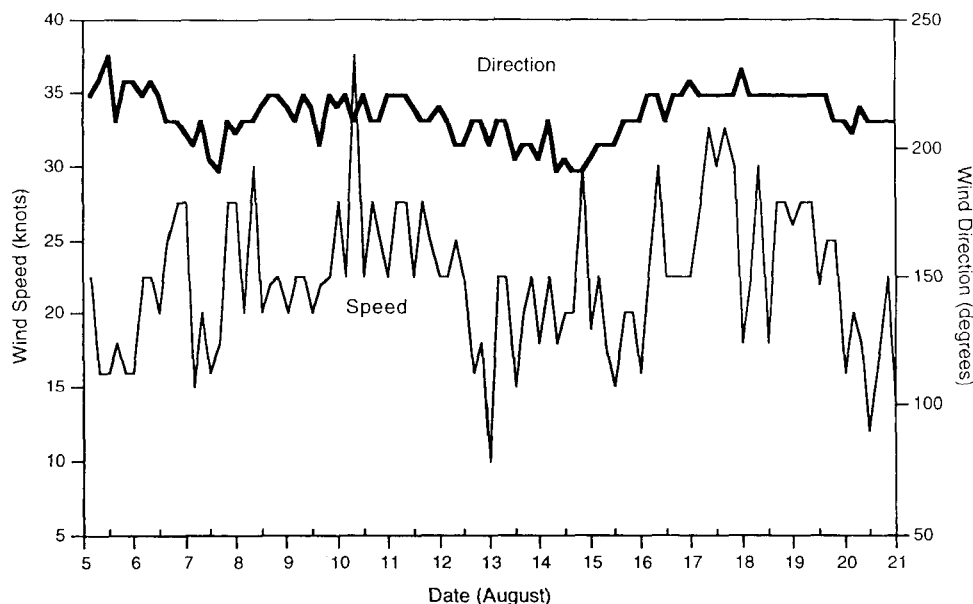


Fig. 6. Corrected wind speed and direction for the duration of the cruise.

stability maximum (Fig. 8c) which arises from bunching of the isopycnals in the frontal zone. The high chlorophyll *a* can be attributed to the phytoplankton being trapped within a shallow mixed layer. This process is the same as that which produces phytoplankton patches on the stratified side of many oceanic fronts (LeFevre, 1986). To the southeast of the high chlorophyll *a* patch the depth at which the chlorophyll *a* concentration declines to $< 1 \text{ mg m}^{-3}$ varies by nearly 40 m, and this depth is clearly correlated with the depth of the stability maximum (Fig. 8c).

Another interesting feature of the chlorophyll section is the tongue of low chlorophyll, at $58^{\circ} 30' \text{E}$, which extends upwards for about 50 m and cuts across isopycnals from σ_{θ} 25.4–25.0. This feature was also seen on legs 3, 5, and 6 and so is not an artifact of the particular leg. It is in the same area as one of the high salinity patches referred to above, although that feature does not involve the apparent diapycnal mixing shown by the low chlorophyll *a* tongue. The fact that the Seasoar legs were separated by up to 25 km suggests that the processes producing this zone of anomalously lower chlorophyll *a* have an along-slope coherence.

3.2.2. Seasoar survey 2

The second Seasoar survey was carried out between 16 and 18 August and time limitations restricted it to a bow-tie shaped pattern including a repeat of the first survey's leg 4, passing through the Arabesque station, and a leg parallel to the bottom contours coinciding with leg 7 of survey 1 (Fig. 9)

A number of major differences between the two surveys were recognizable in the surface temperature and salinity. These will be due partly to advective changes and

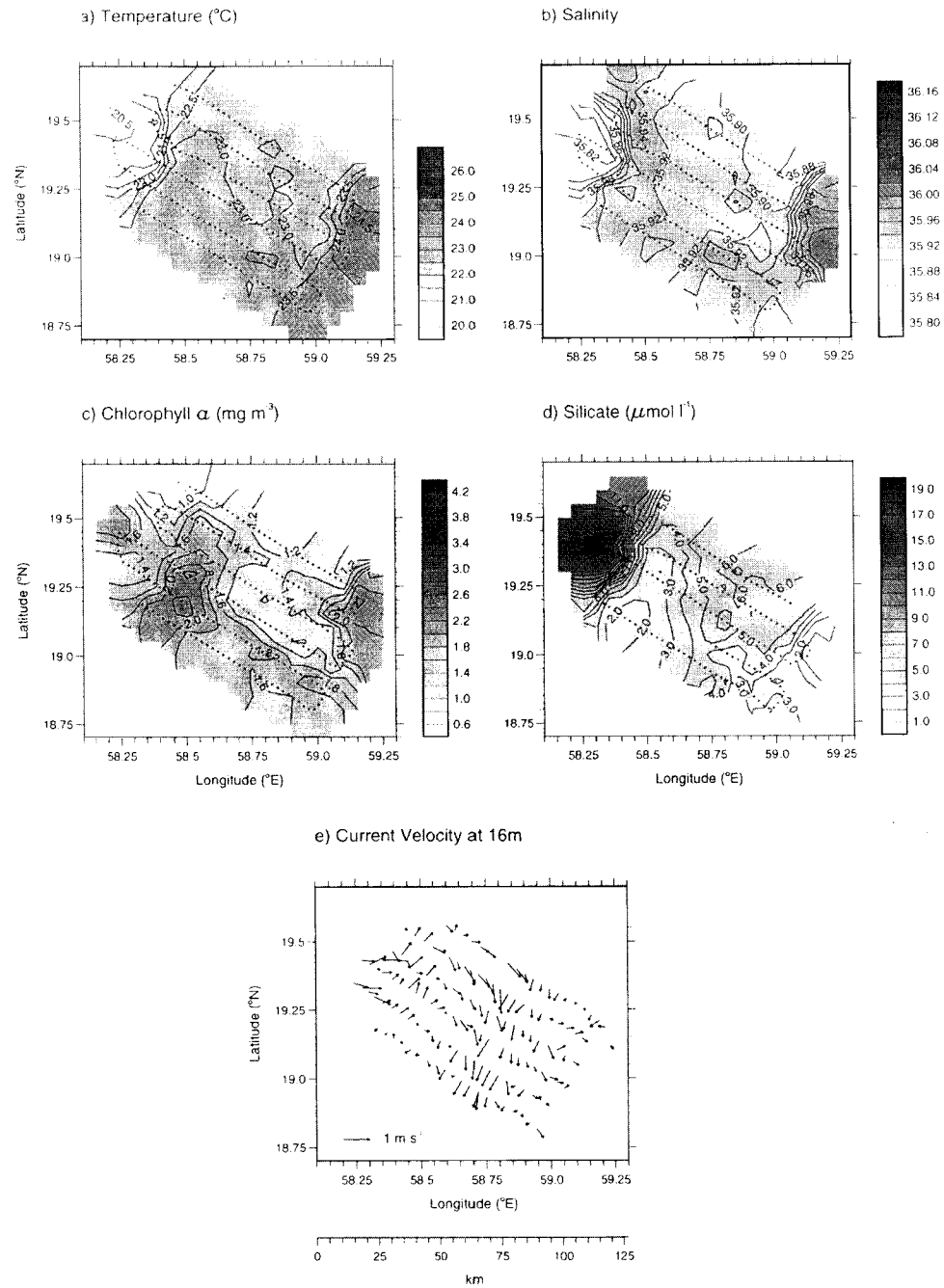


Fig. 7. Surface contoured plots for Seasoar survey 1 (the data were contoured using a 0.05° grid with a 0.1° search radius for the gridding algorithm). (a) temperature, (b) salinity, (c) phytoplankton chlorophyll a (mg m^{-3}), (d) silicate ($\mu\text{mol l}^{-1}$), and (e) ADCP current vectors at 16 m depth. The survey track is indicated by the dotted line.

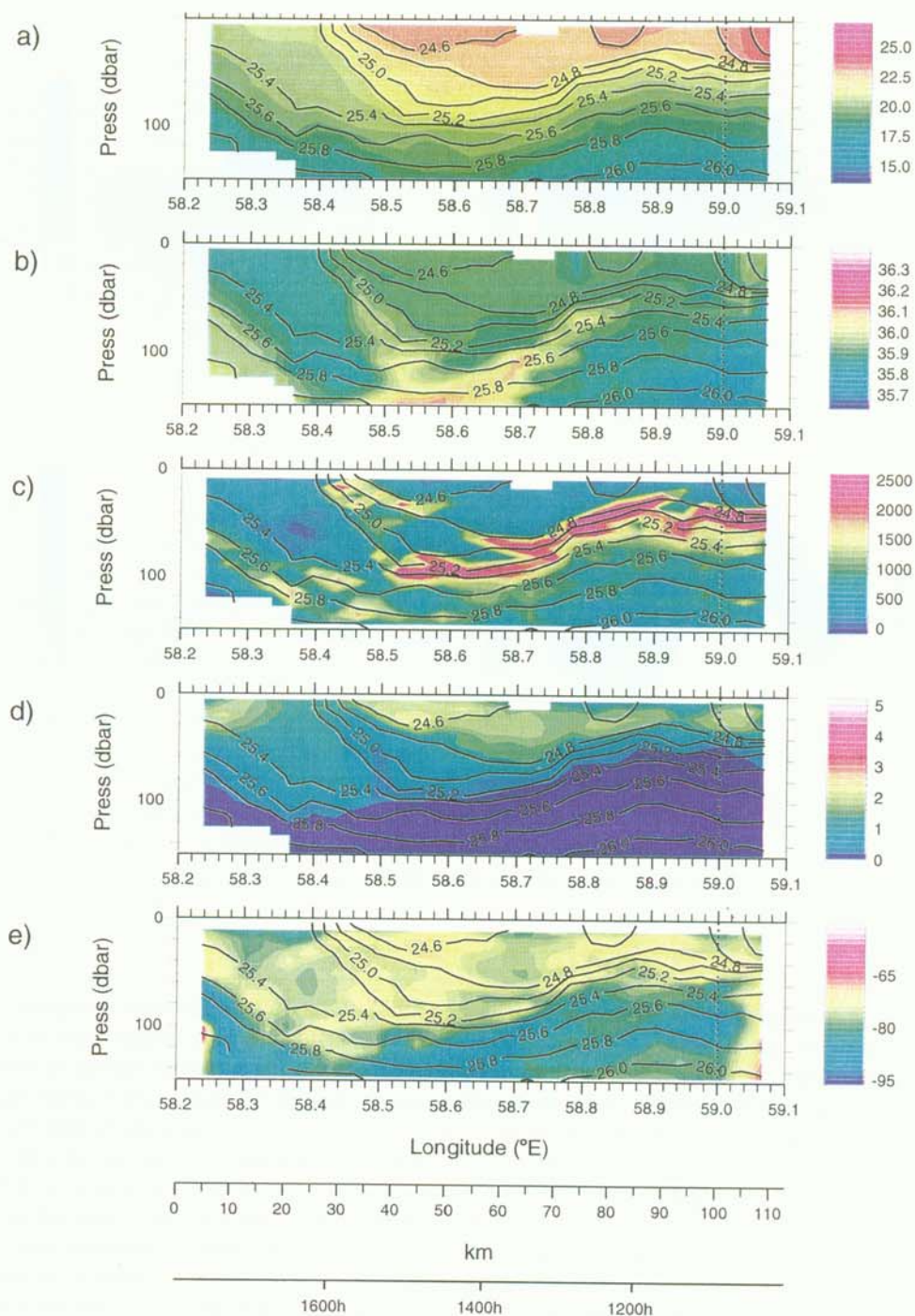


Fig. 8. Contoured Seasoar transects from survey 1 leg 4. (a) temperature, (b) salinity, (c) stability ($10^8 \cdot (dp/dz)/\rho \text{ m}^{-1}$), (d) phytoplankton chlorophyll *a* (mg m^{-3}), (e) absolute ADCP backscatter (dB). Iso-pycnals are superimposed on all plots. Time is local (i.e. GMT + 4). The Arabesque position (59°E) is marked with a dotted line.

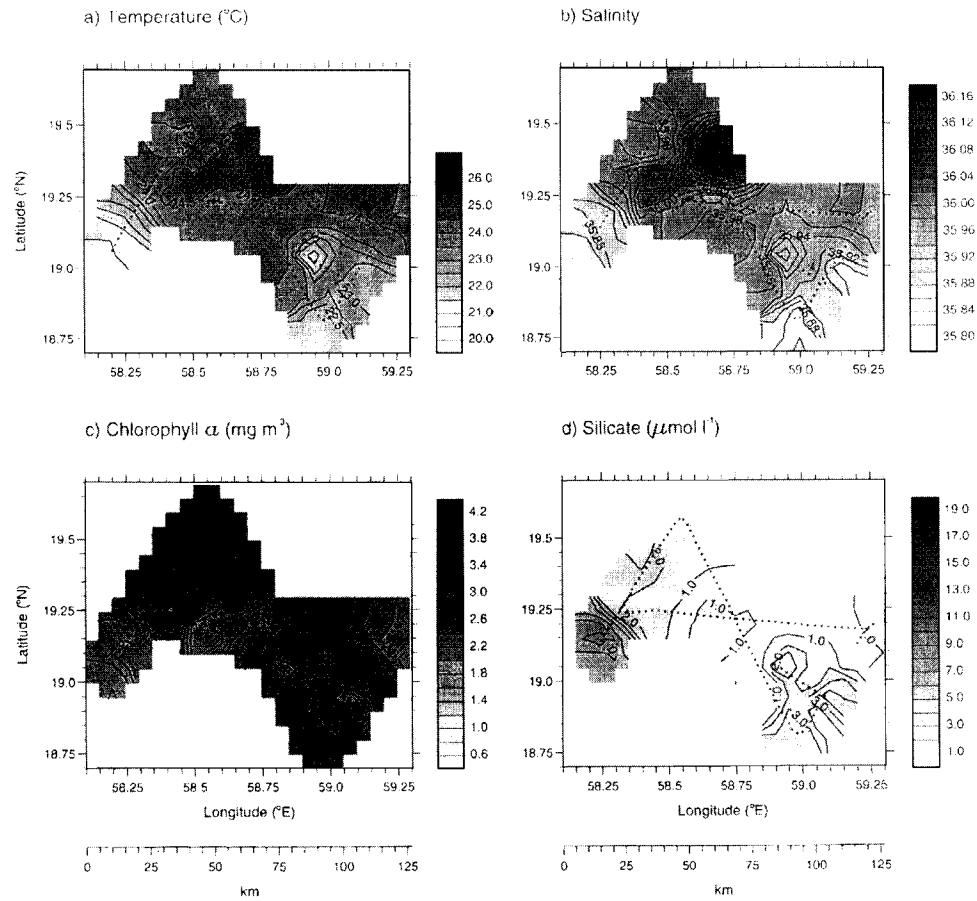


Fig. 9. Surface contoured plots for Seasoar survey 2 (a) temperature, (b) salinity, (c) phytoplankton chlorophyll *a* (mg m^{-3}), (d) silicate ($\mu\text{mol l}^{-1}$). The survey track is indicated by the dotted line.

partly to temporal changes in the physics and biology; the two are difficult to separate because the small observational area will have had a flushing rate of probably only a few days. The small high salinity region observed at the east of survey 1 had disappeared but a patch of very high salinity water (> 36.16) was found along the leg running from southeast to northwest (Fig. 9b). The Seasoar data show that this water was found throughout the mixed layer but we do not know its source. Another difference was that only a trace of cold, newly upwelled water was found at the extreme south of leg 7 (Fig. 9a), but this may have been because the repeat of leg 4 did not extend as far up the slope as during survey 1. This low temperature water still had high silicate values (Fig. 9d) although these were lower ($7 \mu\text{mol l}^{-1}$) than on survey 1 ($14 \mu\text{mol l}^{-1}$). Silicate levels were generally much lower than on survey 1 and chlorophyll *a* values were higher, indicative of diatom growth in the interven-

ing 6 days (see Fig. 12). As on survey 1 the chlorophyll *a* levels were higher on the stratified side of the upwelling front (Fig. 9c).

The Seasoar section for survey 2, leg 4, is shown in Fig. 10 (cf. survey 1, Fig. 8). The main difference between the surveys is the intensification of the shallow seasonal thermocline (Fig. 10a,c). The main concentrations of chlorophyll *a* ($1.5\text{--}5\text{ mg m}^{-3}$) were within the mixed layer, with the highest concentrations at the western (shoreward) end (see also Fig. 9d). Note however that there were moderate levels of chlorophyll *a* ($0.4\text{--}0.8\text{ mg m}^{-3}$) below the main mixed layer, bounded by a band of high stability (Fig. 10c) which was probably a relict pycnocline formed earlier (cf. Fig. 8c).

3.3. Phytoplankton composition

3.3.1. Spatial variability during the first Seasoar survey

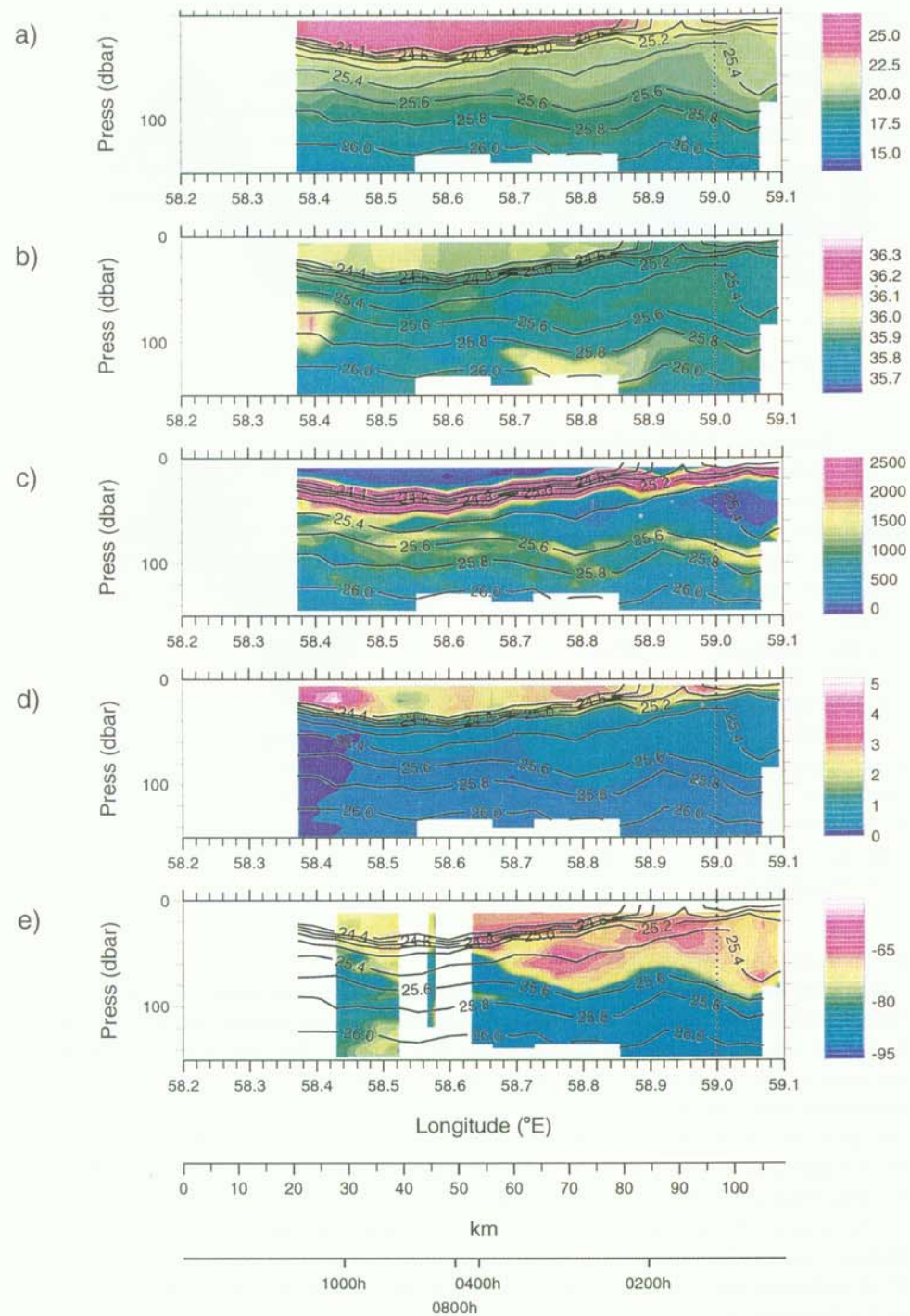
Fig. 1 shows the location of the phytoplankton samples taken from the ship's non-toxic seawater supply system on August 10 (samples A and B) and 12 (sample C). Cells were counted by Derek Harbour (Plymouth Marine Laboratory) and data converted to mg C m^{-3} . Samples A and C are both close to the shelf edge and are similar in their composition of the main taxonomic groups, with $5\text{--}10\text{ mg C m}^{-3}$ for both flagellates and diatoms, $3\text{--}5\text{ mg C m}^{-3}$ cyanobacteria and $< 3\text{ mg C m}^{-3}$ dinoflagellates and coccolithophores (Fig. 11a,c). The surface water temperature was $< 23^\circ\text{C}$ close to the shelf, but higher offshore; nutrient levels, as indicated here by silicate, were relatively high ($> 10\text{ }\mu\text{mol l}^{-1}$).

In sample B, at the eastern corner of the survey, the diatoms and dinoflagellates were approximately twice as abundant as in A and C, whereas the flagellates were similar in quantity (Fig. 11b). Sample B was from close to the front bordering the North Arabian Sea surface water (Fig. 7a) and the inorganic silicate at the site was only half that at the locations of samples A and C, correlating with the higher diatom abundance.

3.3.2. Temporal variability

Samples were taken to a depth of 100 m at the Arabesque reference station (19°N , 59°E) on August 5 and 21. These are shown as depth profiles of the taxonomic groups of phytoplankton and heterotrophs (Fig. 12a,b). The data show that between the surface and 30 m the phytoplankton carbon doubled between the two dates, commensurate with equivalent increases in the cyanobacteria, flagellates and diatoms. The profiles for the heterotrophs show a 3-fold increase in biomass to a depth of 50 m, largely due to the increase in the heterotrophic dinoflagellates. Ciliates declined by approximately a third over the same period.

The change in biomass is also observed in the chlorophyll *a* data for the two Seasoar surveys, probably as a result of the vertical density difference in the upper 50 m following an increase in surface heating. The Seasoar transects show a shoaling of the layer of maximum stability.



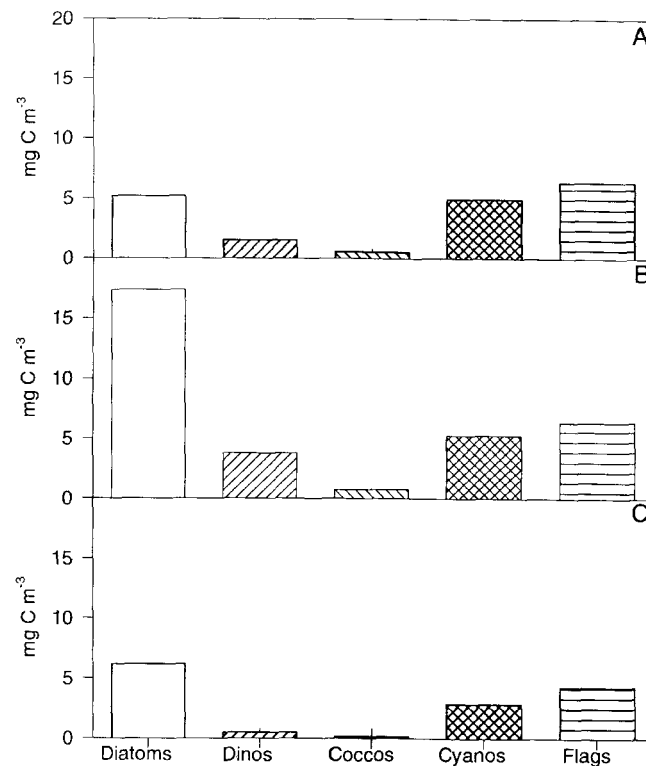


Fig. 11. Carbon concentration of the major floristic groups from three surface samples taken during Seasoar survey 1 at the positions (A, B and C) shown in Fig. 1.

3.4. Acoustic backscatter

The ADCP data for the entire cruise are available in Roe et al. (1995). Here we illustrate the main features of interest.

3.4.1. Diel vertical migration

Fig. 13 shows a section taken over 48 hr during Seasoar survey 1. The time scale on all figures is GMT; local time is GMT + 4, so night is shown here as ca 1500–0300 hr GMT. Local night was coincident with those tracks which crossed the continental shelf.

Fig. 10. Contoured Seasoar transects from survey 2, leg 4. (a) temperature, (b) salinity, (c) stability ($10^8 \cdot (dp/dz)/\rho \text{ m}^{-1}$), (d) phytoplankton chlorophyll *a* (mg m^{-3}), (e) absolute ADCP backscatter (dB). Isopycnals are superimposed on all plots. Time is local (i.e. GMT + 4). The Arabesque position is marked with a dotted line.

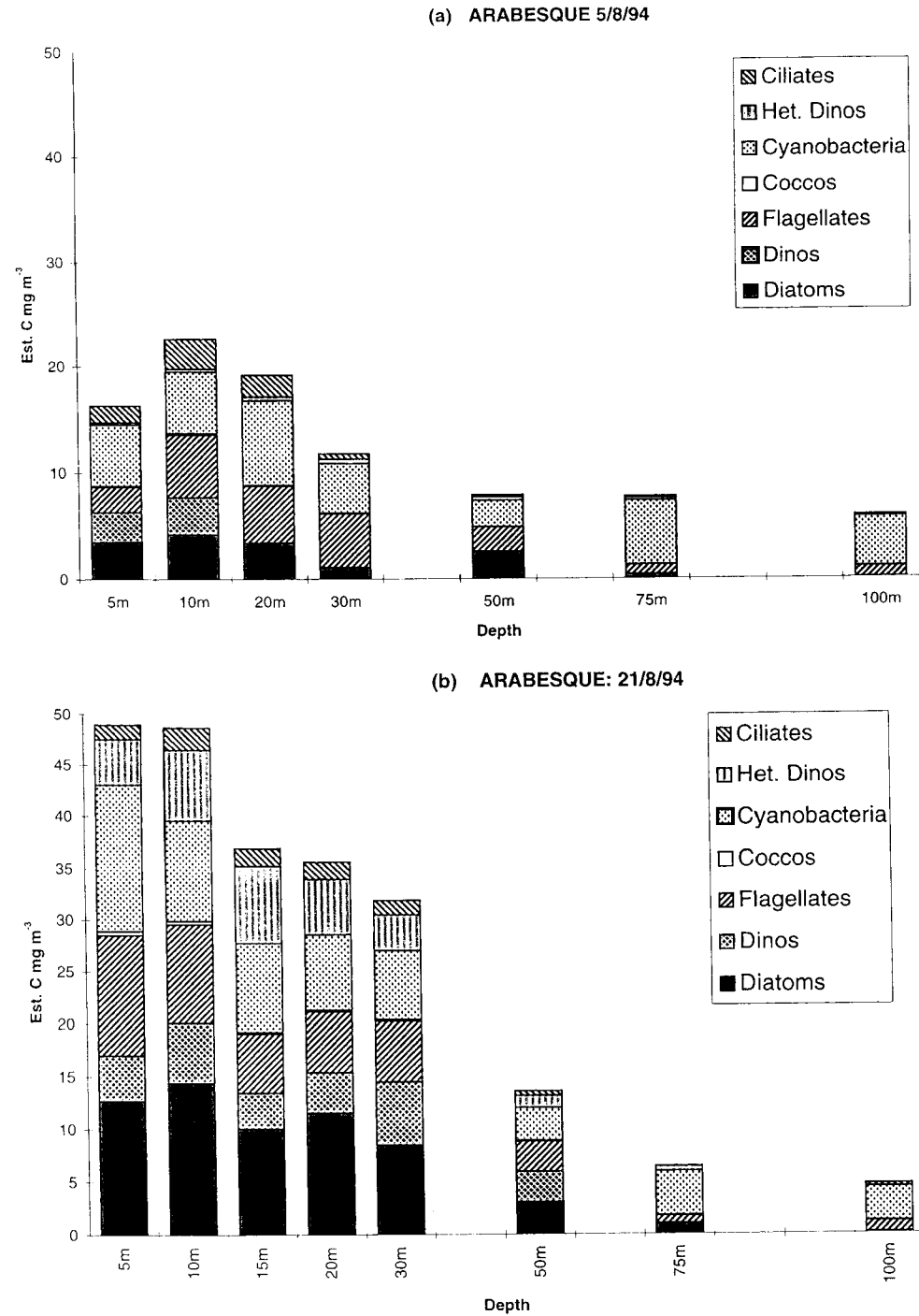


Fig. 12. Taxonomic composition of phytoplankton and heterotrophic groups at the Arabesque reference station on (a) 5 August and (b) 21 August 1994.

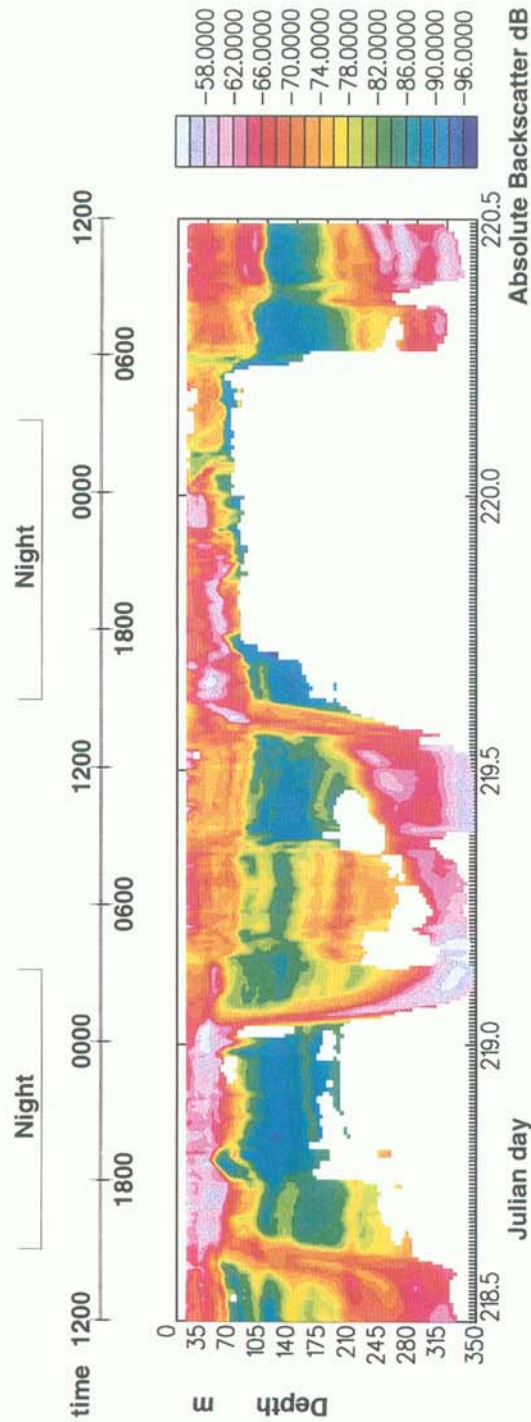


Fig. 13. MVBS data from the ADCP over the whole 48 hour period of Seascope survey 1, with time in GMT (local time — 4 hours). Two distinct diel migrations are shown typical of those observed during the cruise. Local night-time is coincident with crossing the continental slope.

Two distinct diel migrations are shown which are typical of the pattern seen throughout the cruise. There are very large dynamic ranges in dB (from < -56 dB to > -98 dB) with marked layering of backscatter, some of which is coincident with the oxycline at 70–100 m. At night high levels of backscatter occur above the oxygen minimum layer and only very low levels within it. This marked diel periodicity in the levels of backscatter within the layer reflects the low numbers of animals (= acoustic targets) which are present during the night at these depths. The levels of backscatter at night are so low that they approach the noise level of the system and these data are rejected because they do not meet the criteria of 25% good (see Roe et al., 1995 for details).

During the day there were high levels of backscatter between the surface and 70 m (above the oxygen minimum) as well as layers and patches of high backscatter within the oxygen minimum layer. The populations responsible for this deep backscatter clearly move up above the oxycline at night. These overall backscatter patterns mirror the RMT8 catches and to some extent the RMT1s (Figs. 17 and 18). Highest volumes occur in the surface 100 m during the day and night, with secondary daytime peaks at depths of 200–400 m. At night the volumes below 100 m were very low (see below).

3.4.2. Multiple layering

The most remarkable feature of the ADCP backscatter data was the occurrence of very finely resolved multiple scattering layers during the day. The left side of Fig. 14 shows backscatter data taken 0700–0900 h August 6, in which there are

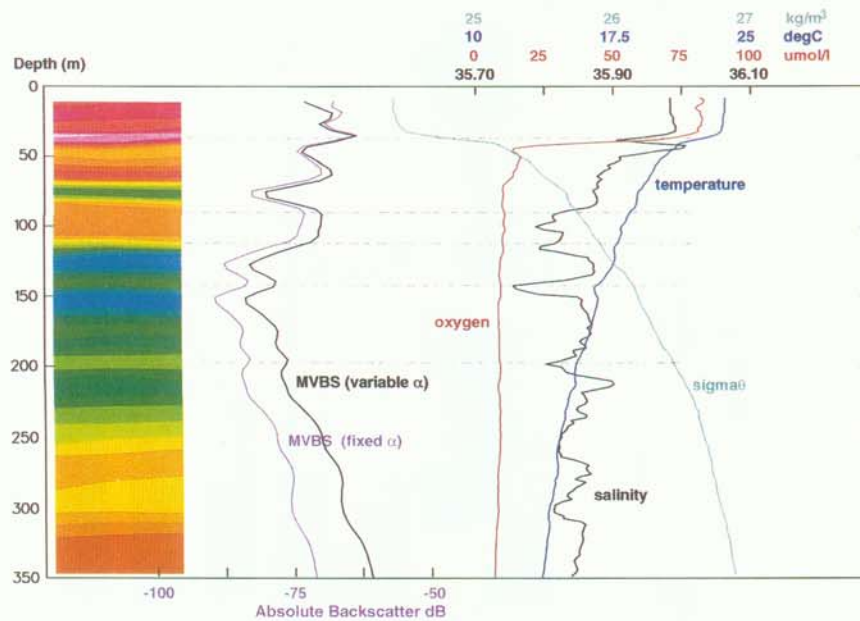


Fig. 14. MVBS data from the ADCP taken over a 2 hour period coincident with a CTD station. Multiple layers in the MVBS data in some cases (50 m–200 m range) correspond with variability in the salinity profile.

distinct multiple layers in the upper 350 m (the MVBS curves to the right of the contoured section are derived from the average over the 2 hour period). These layers vary in thickness from < 10 m to ca 100 m. MVBS varied dramatically between the layers, e.g. at ca 75 m (the depth of the oxycline) there is a layer of ca -82 to -84 dB sandwiched between layers of -68 dB above and -72 dB below. Note that a 3 dB difference in backscatter represents a doubling of the signal strength (which in turn is an indication of biomass).

Data from a CTD down cast concurrent with the backscatter data are shown in the right-hand side of Fig. 14, alongside the MVBS curves which were calculated using both a fixed value for absorption (α), and with α corrected for temperature and salinity using the equations of Francois and Garrison (1982). The corrected MVBS curve highlights the effect of temperature on sound absorption; the distance between the fixed α and variable α curves increases with depth and decreasing temperature.

The CTD salinity profile shows variability which at some depths seems to be related to the backscatter layering, or variability in Sv (decreases in salinity corresponding to increases in backscatter). In order to quantify this apparent relationship, a cross-correlation analysis was applied to the salinity and corrected MVBS data after pre-whitening the spectra to eliminate any spurious correlations. The resulting correlation peak ($r = -0.48$) was found to be offset by 4 metres (i.e. salinity lagging by one depth cell). Accepting this offset, however, and testing significance using Student's t distribution with a 5% significance level and our 36 observations, we conclude that our value of r is much higher than that required (~ 0.3) to accept the hypothesis ($H_0: \rho \neq 0$), i.e. that there is a significant correlation. From the density curve, σ_θ , there is no evidence to suggest that backscattering is occurring as a result of physical turbulence, except in the region of the thermocline.

We have observed similar fine scale layering on a more recent cruise (February 1997) in the Gulf of Oman, but have yet to make further detailed comparisons with concurrent CTD data.

3.4.3. Relationship with Seasoar data

Coupling the Seasoar hydrography with acoustic backscatter from the ADCP allows us to examine the relationships between the zooplankton biology and the physical environment, at vertical scales of 4 m and horizontal scales of ca 4 km. The example shown here (Fig. 15) is the Seasoar section (leg 4) described earlier (Fig. 8) but here extended to a depth of 350 m to include the deep observed backscatter. The section was taken between ca 1000–1800 h local time (0600–1400 GMT), i.e. essentially during the day, with dusk coinciding with arrival on the continental slope. Backscatter is highest above the slope but throughout the section there are patches of relatively high backscatter which are associated with high chlorophyll levels ($> 0.6 \text{ mg m}^{-3}$, see Fig. 8d,e). Below this there is a layer of very low backscatter (< -78 dB) and then a layer of high backscatter (> -69 dB) below 240 m and within the oxygen minimum layer. Essentially Fig. 15 reflects the daytime situation in Fig. 13, with backscatter maxima both within the oxygen minimum layer and in the surface mixed layer.

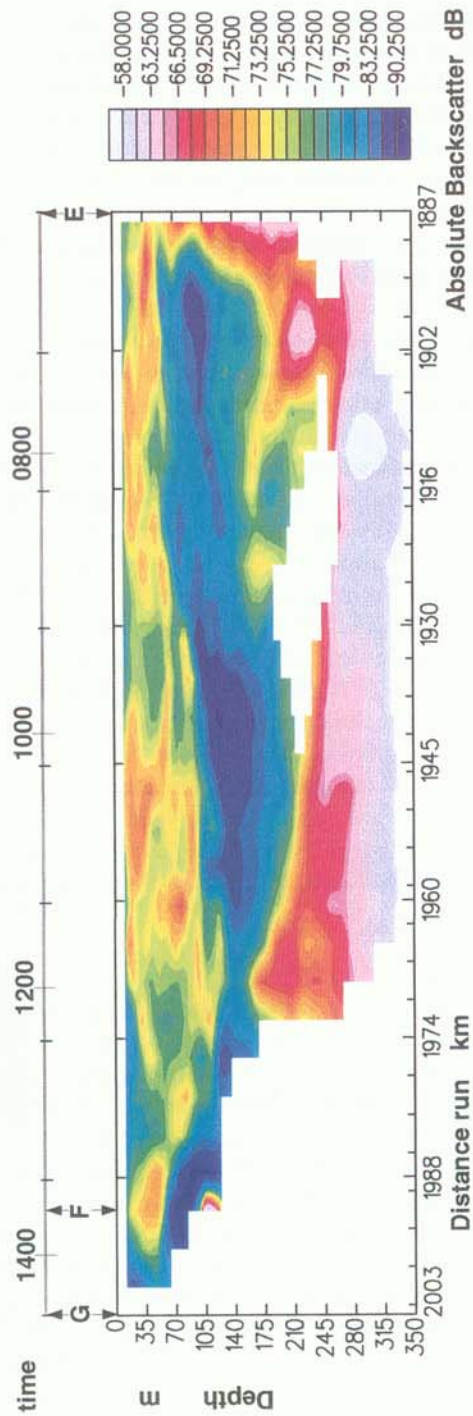


Fig. 15. Absolute Backscatter data taken from SeaSoar survey 1, leg 4, with time in GMT, showing high backscatter on the continental slope, patchiness near the surface, and very low levels below the oxycline and the lower limit of the euphotic zone. Levels increase sharply below ~240 m depth. The section between E and F marks the extent of leg 4 and F to G covers the turn towards leg 5 (see Fig. 1)

3.5. Biomass data

3.5.1. Mesozooplankton (LHPR samples)

The two LHPR data sets from the Arabesque reference station both have high biomass levels in the upper 100 m (up to 3 ml m^{-3} , equivalent to $> 200 \text{ mg}$, or 17 mM, C m^{-3}), and very much lower ones between 100 m and 250 m, i.e. below the oxycline (Fig. 16). In the second data set there is an increase in the volume of six samples between 164 m and 195 m on the down run. This was caused by simultaneous increases in the densities of several groups (euphausiids, chaetognaths, decapods and ostracods) and did not occur during the up run.

3.5.2. Macrozooplankton (RMT1 samples)

The damage to the fine mesh nets caused by the rough seas meant that the depth profiles of macrozooplankton at all three stations were incomplete (Fig. 17). The samples have not been sorted and the relative contribution of gelatinous and non-gelatinous taxa has only been assessed qualitatively. Because of this no attempt has been made to convert the biovolume data to carbon.

At the Arabesque station, only one deep and three near-surface samples contained large volumes of material, and the contributory taxa were different in each case. The 0–50 m night sample contained phytoplankton aggregates that made a significant contribution to the volume of $1588 \times 10^{-3} \text{ ml.m}^{-3}$. In the 50–100 m depth range the day haul was dominated by the medusa *Pelagia*, while the night haul consisted mainly of copepods, small fish, euphausiids and phytoplankton aggregates. A single large medusa dominated the biovolume of the 900–1000 m day sample.

At the slope station (Fig. 17) the volumes of the samples were very low in comparison with the other two stations. This resulted from the relative absence of medusae. However, no samples were obtained in the 0–50 m depth range. The samples generally comprised small copepods and euphausiids, with some foraminiferans, particularly at the shallower depths. Below 100 m depth the night catches were unaccountably considerably smaller than the day ones. The difference does not appear to be the result of diel vertical migration.

At the shelf station (Fig. 17) the biovolume of the samples increased dramatically in comparison with the slope station. The two day hauls again were considerably larger than their night counterparts, and were dominated by the medusa *Pelagia*. This medusan was also present in the night hauls, but in far smaller numbers. The 0–50 m night haul contained mainly small copepods and euphausiids, with some decapods, foraminiferans and phytoplankton aggregates.

3.5.3. Micronekton (RMT8 samples)

The depth distribution of biovolume and carbon for the gelatinous, mainly cnidarian, and non-gelatinous taxa at the three stations sampled are shown in Figs. 18 and 19 respectively. At the Arabesque station, the volumes of the four samples in the top 100 m of the water column were considerably higher than at greater depths (Fig. 18). This is clearly a reflection of the presence of the oxycline, with very low oxygen values between 100 and $\sim 1100 \text{ m}$ depth (Fig. 2b). As was the case with

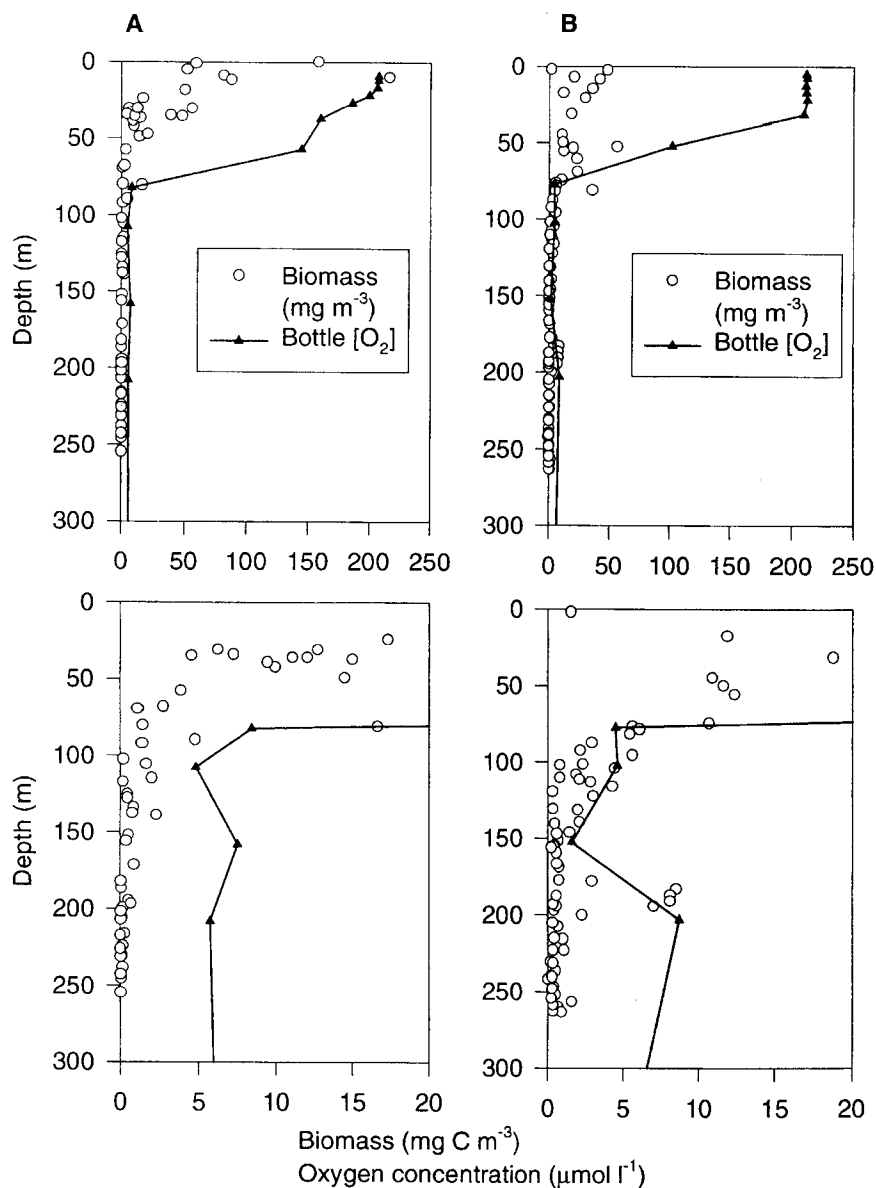


Fig. 16. Vertical profiles of mesozooplankton from LHPR samples and CTD oxygen at the oceanic (Arabesque) station at (A) 1950 local time on 12 August and (B) 0900 local time on 21 August. The lower figures show an expanded scale plot of the same data.

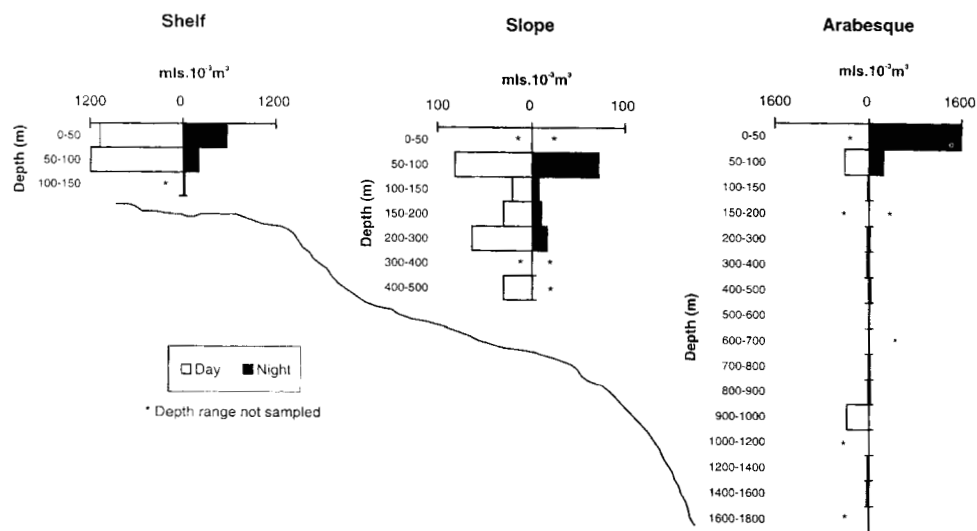


Fig. 17. The day and night vertical distribution of RMT1 biovolume (ml per 10³ m³) at the shelf, slope, and oceanic (Arabesque) stations.

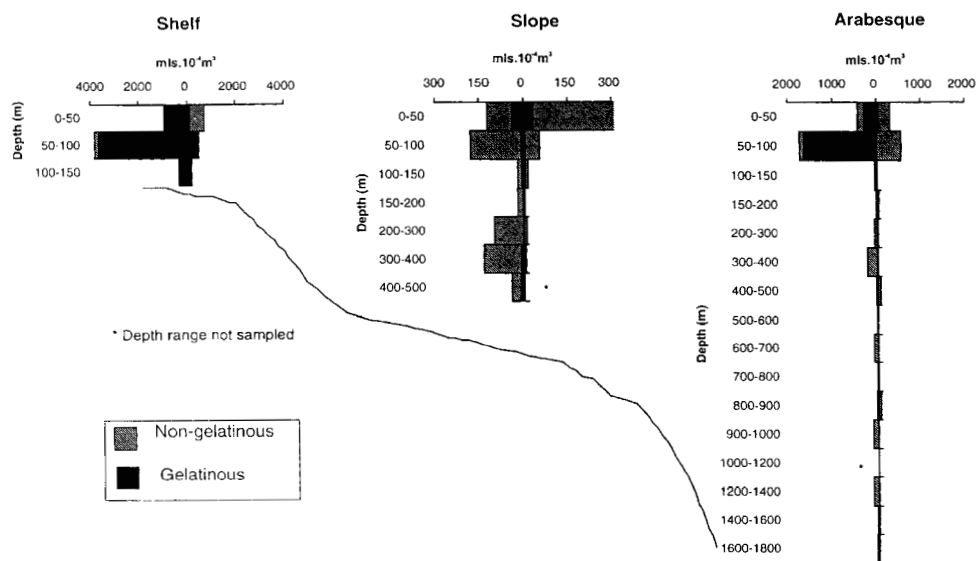


Fig. 18. The day and night vertical distribution of RMT8 gelatinous and non-gelatinous (other) biovolume (ml per 10⁴ m³) at the shelf, slope, and oceanic (Arabesque) stations.

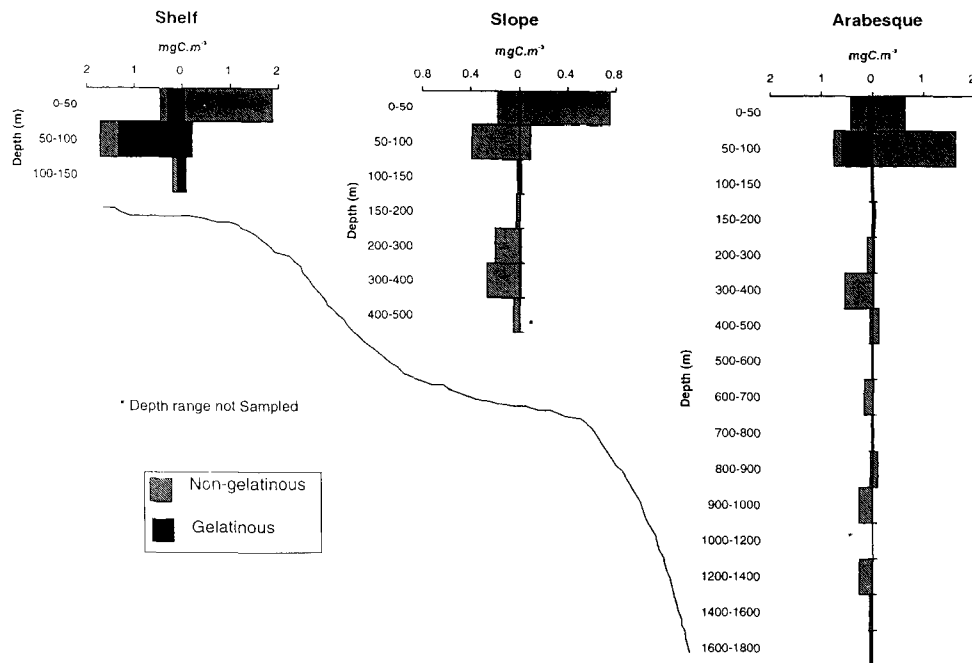


Fig. 19. The day and night vertical distribution of RMT8 gelatinous and non-gelatinous (other) carbon (mg m^{-3}) at the shelf, slope, and oceanic (Arabesque) stations.

the matching RMT1 samples, there were differences in the main contributors to each sample. *Pelagia* was the main contributor to the two day hauls, although its numerical abundance differed (Fig. 20). It dominated the 50–100 m sample, making up almost 98% of the total numbers, whereas it contributed only ~16% of the numbers in the 0–50 m range, where small chaetognaths and siphonophores contributed 55% and 24% respectively. *Pelagia* was almost entirely absent from the night hauls, indicating a great deal of patchiness in its distribution in the area. A single large squid (*Symplectoteuthis oualaniensis*) contributed two-thirds of the volume of the 50–100 m night sample, such that the overall number of specimens of all taxa was relatively low (Fig. 20) whereas the total carbon was relatively high (Fig. 21). The 0–50 m night haul had a very diverse composition, with siphonophores, chaetognaths, decapods and euphausiids respectively contributing 20%, 28%, 15% and 20% of the total volume, and 34%, 38%, 5% and 16% of the very large ($> 20,000$ per 10^4m^3) total number of individuals. However, because of the great number of small siphonophores, the total carbon was very similar to that of the 0–50 m day haul (Fig. 21) where the total population number was ~3700 individuals per 10^4m^3 (Fig. 20).

Below 100 m the volumes of the samples were generally low. This correlates with the ADCP data which indicate a lack of backscatter below the oxycline. The main contributors to each sample varied considerably (Fig. 20). During the day medusae and siphonophores dominated the 100–200 m depth range, while at night the popu-

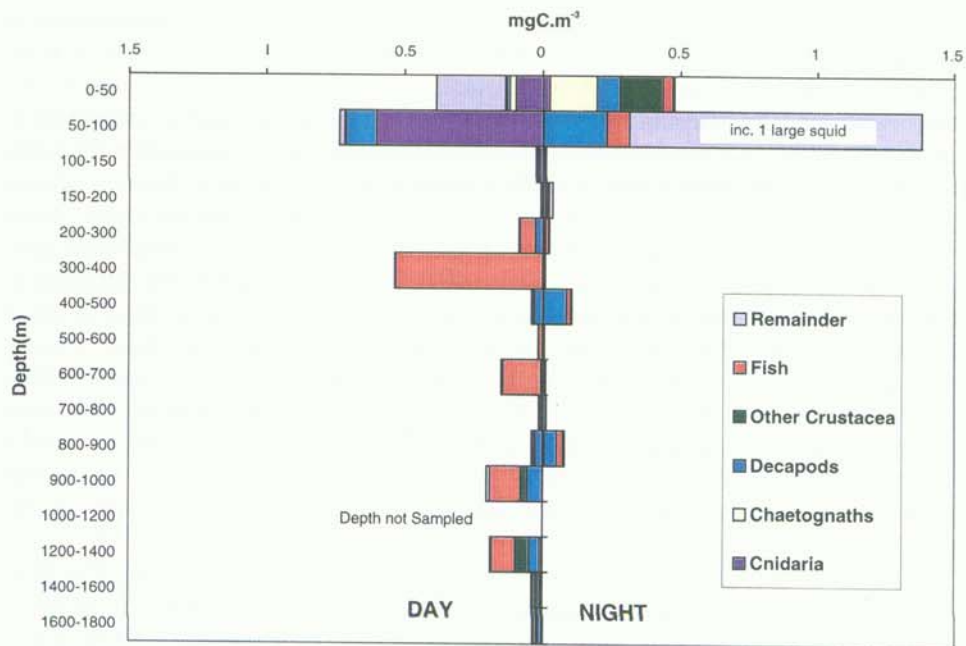


Fig. 20. The day and night vertical distribution of numerical abundance (nos per 10^4 m^3) of particular taxa in the RMT8 samples from the oceanic (Arabesque) station.

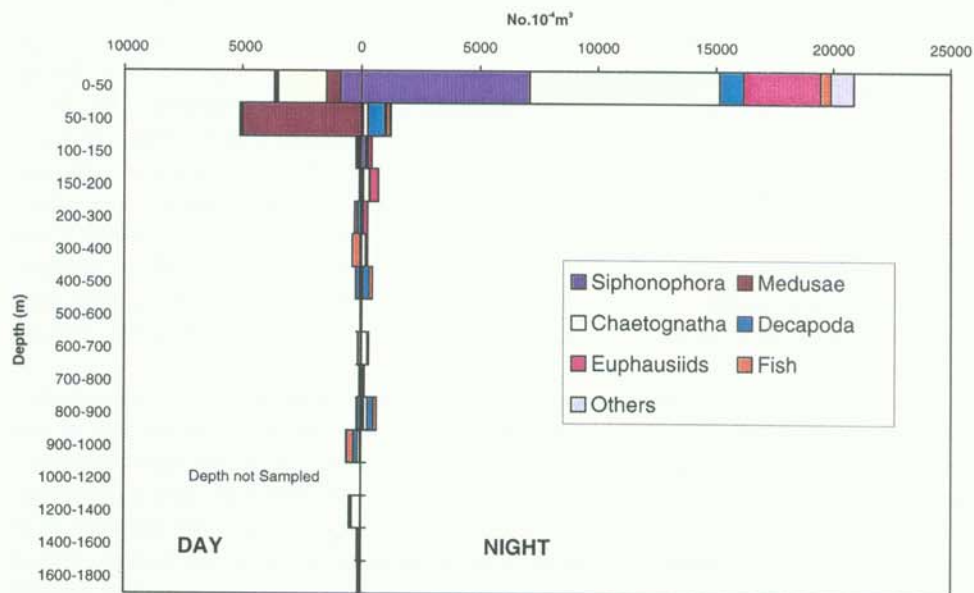


Fig. 21. The day and night vertical distribution of RMT8 carbon (mg m^{-3}) in different taxa at the oceanic (Arabesque) station.

lation was more mixed. Below 200 m decapods and fish (particularly species of the myctophid genera *Diaphus* and *Hygophum* and the photichthyid *Vinciguerria*) were the main components. By day fish were usually more numerous than decapods, but at night decapods (particularly species of *Gennadas*, *Plesionika* and *Sergestes*) were the greater contributors to the biovolume. The relatively large contribution made by fish to the day hauls meant that the carbon content of some of these deeper samples was quite significant, and in one instance the C concentration exceeded that in the upper 50 m of the water column (Fig. 21). Cnidarians tended to be more abundant during the night, while tunicates were extremely rare at this station and, apart from a single salp, were represented by only a few small doliolids. The general absence of tunicates can be related to the presence of the swarms of *Pelagia*. These animals are known to feed on a variety of gelatinous organisms (Larson, 1987; Malej, 1989) including tunicates (L.P. Madin, personal communication). The integrated volumes in the top 900 m of the water column at the Arabesque station were 15.91 ml.m^{-2} by day and 6.79 ml.m^{-2} by night. The difference was almost entirely due to the swarms of *Pelagia* encountered in the top 100 m by day, but which were absent during the night hauls.

At the slope station the volumes of the samples were considerably smaller than those at the Arabesque and shelf stations (as was the case for the RMT1 samples), due to the virtual absence of large medusans (Fig. 18). As a result the depth distribution of carbon (Fig. 19) closely reflects that of biovolume. The integrated volumes in the 0–400 m depth range were 4.5 ml.m^{-2} by day and 2.09 ml.m^{-2} by night, as compared with 13.89 ml.m^{-2} and 5.12 ml.m^{-2} , respectively, for the same depth range at the Arabesque station. The percentage of this biovolume in the top 100 m increased from 30% by day to 90% at night. The 0–50 m night sample was taxonomically very diverse, with 29 specimens of the swimming crab *Charybdis smithii* contributing 30% of the total volume. The haul also contained ~ 13,000 chaetognaths. This diversity of taxa also applied to the other hauls in the 0–100 m depth range, with the differences in volume being largely due to the number of swimming crabs present (Van Couwelaar et al., 1997). At greater depths the day hauls mainly comprised small euphausiids, decapods and fish, with chaetognaths also being numerically important. The first three of these taxa largely migrated into the top 100 m at night, so that the night volumes of the samples in the 100–400 m depth range were very small. Doliolids were more abundant at this station, possibly reflecting the scarcity of *Pelagia*.

At the shelf station *Pelagia* was the predominant organism, but its distribution was patchy and more specimens were taken by day (13 litres in the 50–100 m day haul) (Fig. 18). Swimming crabs were also relatively numerous in the upper 100 m by day and 50 m at night. The 100–150 m day haul also contained many small decapods, euphausiids and pteropods. These migrated into the top 50 m at night, together with some fish whose day depth distribution was presumably close to the bottom, below the sampling depth. This migration resulted in a large increase in the carbon content of that sample (Fig. 19).

4. Discussion

The water masses involved in the circulation patterns of the region are well known and have been summarised by Currie (1992). The Persian Gulf Water is particularly clearly demarcated in the study area. The CTD transects show that off the Omani coast the PGW has a limited horizontal extent (Fig. 3). In the northern transect it begins to peter out east of 59.4° E. The stations on the slope are not spaced closely enough to determine whether the PGW extends right up to the slope. However the IIOE data shown by Currie (1992), Fig. 7, suggests that it does not, and that water of salinity 35.7–35.8 lies between the PGW and the coast. The northern transect also shows a patch of high salinity water (> 36.0) above 100 m at σ_θ values of 25.4. CTD data obtained from *RRS Charles Darwin* in 1986 at the mouth of the Gulf of Oman (Currie, 1992) show that high salinity water at these densities was present in this area and is presumably the source of this water off the Omani coast (see also the Seasoar sections). Currie (1992) found that PGW did not appear to be present in all IIOE sections and he suggested that the southern flow of PGW might be inhibited by the southwest monsoon. Our more extensive data do not support this view.

While the PGW provides a major mid-depth feature in the study area, the near-surface characteristics are more variable. Between the upwelled water to the southwest and the North Arabian Sea water at the northeastern corner of the box was the large area of variable silicate and chlorophyll *a* concentrations and the ADCP current vectors (Fig. 7e) indicate a possible origin for this water. The most prominent feature was an area of high currents (1–1.5 kt) which flow southeast in the northern part of the survey and then swing round to the southwest to pass through the centre of the area with low temperature gradients. This current can be identified with the sloping isopycnals on the Seasoar section between $58^\circ 35'W$ and $58^\circ 50'E$ (Fig. 8). The zone of high silicate ($4\text{--}6 \mu\text{mol l}^{-1}$) and lower chlorophyll *a* concentrations can be identified with this advective feature. Some of this water between the two frontal zones may therefore have originated as a filament of upwelled water that was advected away from a coastal source somewhere to the north of the survey area. Support for this contention comes from an AVHRR satellite image of the area obtained on August 9 (Kindle et al., 1996). This shows a small area of low temperature water in the same area as the 20°C water in the west of our survey. It also shows an area of cold upwelled water 50 km to the north of the survey and the temperature pattern suggests that this water was being advected southwards into the survey box in the region of the high southward currents recorded by the ADCP.

A small patch of high chlorophyll *a* was found in the upwelling area during the first survey (Fig. 7c). The Seasoar data show that this is associated with a zone of marginally higher stability at the depth of the 25.4 isopycnal (Fig. 8c). However, even in the centre of the upwelling zone (between σ_θ values of 25.2 and 25.4) the chlorophyll *a* values are considerably higher ($0.6\text{--}0.8 \text{ mg m}^{-3}$) than was found between these density surfaces away from the upwelling area ($< 0.2 \text{ mg m}^{-3}$). This suggests that the time scale for the upwelling is long compared with the time scale

of phytoplankton growth and therefore that significant growth can occur during the time taken for the upwelling water to reach the surface.

The absolute backscatter from the ADCP (Fig. 8e, Fig. 15) can be regarded as a measure of zooplankton/micronekton biomass in the ~ 10 mm size range, although there is no simple linear relationship. With the exception of the two deep areas of high backscatter at each end of the section, the areas in which backscatter is > -70 dB are confined within those surface areas with chlorophyll values > 0.6 mg m $^{-3}$. This is highlighted by the fact that the base of the high backscatter zone is correlated with the isopycnals. Since the oxycline depth is also correlated with the isopycnal depths (Fig. 4) we conclude that the observed pattern of backscatter is due to zooplankton actively aggregating within the surface oxygen maximum. High backscatter above the 24.8 isopycnal is generally correlated with high chlorophyll, perhaps indicative of a spatial predator-prey linkage between zooplankton and chlorophyll. The multiple layering noted on the ADCP data is not clearly related to the distribution of particular species in the trawls and the correlation with salinity changes suggests a physical (or associated particulate) cause. Specific animals (e.g. swimming crabs) may contribute to the overall patterns (Schalk and Van Couwelaar, in Baars, 1994) but we have observed the same multiple layering in the Gulf of Oman, a region from which the crabs were absent.

The phytoplankton and heterotroph distributions and abundances changed markedly between the two sampling periods. Some of the changes (e.g. in the diatoms) are a predictable gross consequence of the effects of nutrient-rich upwelling, either offshore or coastal. Others are less easily interpreted. Thus, the order of magnitude increase in heterotrophic species of dinoflagellate, and the expansion of autotrophic ones throughout the water column, in the 16 days between the first and second visit to the Arabesque station, is probably due in part to the vertical mixing produced by the strong winds and in part to the complex interactions in species succession, with superimposed advective effects. A separate sample taken at the time of the first visit and analysed for dinoflagellate species contained only 8 species of dinoflagellate in the upper 50 m (with *Ceratium furca* predominant), while at the second visit the sample had 32 species with *C. candelabrum*, *C. breve* and *C. massiliense* also numerous and an increase in the numbers of *Protoperdinium* spp. The increase in diatoms represented an increase in the abundance of specific types (e.g. of *Rhizosolenia*) rather than an increase in overall taxonomic variety.

The marked differences in the surface water characteristics, identified by the Sea-soar surveys within the very limited area of the survey box, demonstrate the variability faced by the biological populations, from phytoplankton to zooplankton and micronekton. The surface structure is very variable in both time and space; upwelling in the area is not a continuously steady (albeit seasonal) process when examined on the scales at which we have worked. Satellite imagery confirms the locally dynamic nature of the process. However, the large-scale synoptic view of the environment provided by such sources is very different from that experienced directly by the individual organisms in the region. In practice the severity of the oxygen minimum compresses the habitable volume for most species into a thin surface layer where both visual and non-visual predation pressure will potentially be intense. Those few

that are able to exploit the low oxygen layer for at least part of any 24 hr period have the potential advantage of access to a refuge from much of this predation pressure. Alldredge et al. (1984) have suggested that this may account for a layer of diapausing *Calanus pacificus* at the interface with the hypoxic water in the Santa Barbara basin. Normal diel migrants who cannot cope with the hypoxic conditions will not survive in the region unless they adjust their migration behaviour (Judkins, 1980; Longhurst, 1967). Those few who can will have access to the enhanced production of the upwelling-enriched surface waters. Studies of zooplankton distributions have shown how relatively few species thrive in these circumstances; those that do (e.g. *Pleuromamma indica*) may be very abundant (Vinogradov and Voronina, 1962). The same applies to the micronekton; only 1 in 4 of the equatorial species of midwater fish in the Indian Ocean penetrates north of 15°–18°N (Cohen, 1973). Data on other midwater groups in the area are largely lacking.

Our biological samples show how a few species can dominate the area for at least a limited period. During the time we occupied the site swimming crabs and gelatinous species, particularly swarms of *Pelagia*, were very abundant. Gjosaeter (1984) also reports jellies as an important component of several of his trawl samples. This dominance of a few gelatinous species within each group (particularly in coastal samples) has been remarked previously (e.g. Ignat'ev, 1995, reports “during the summer monsoon the content of jellyfish residues...is high”) and the significance of gelatinous animals during the Southwest Monsoon may be a seasonal feature (Madhupratap et al., 1990). Our vertical distributional data for the oceanic station (Figs. 20 and 21) emphasise that the importance of gelatinous species in the top 100 m can be indicated either by their relative numbers (e.g. siphonophores by night, Fig. 20) or by their biomass (gelatinous species by day, Fig. 21). The RMT1 biomass is highest in the upper 100 m, by day and by night, and the LHPR samples of the smaller mesozooplankton emphasise this distribution. The RMT1 biomass values are incomplete but interpolation using the existing data produces integrated values in the top 1000 m at the oceanic station of 90 ml m⁻² (day) and 106 ml m⁻² (night) (Herring and Hargreaves, 1998). Ropke et al. (1993) obtained mean values of 100–150 ml m⁻² in March and April from the top 150 m at a position just north of our sampling site (their “Biobox 1”), using a similar mesh size, while Koppelman and Weikert (1997) with the same mesh found levels of 22 g m⁻² wet wt by day and 37 g m⁻² wet wt by night for the top 150 m of their most western Arabian Sea station (“WAST”). The top 150 m of our data set yield day and night values of 42.2 and 91.9 ml m⁻² respectively. These are not significantly higher than the equivalent values reported for the temperate eastern North Atlantic Ocean in spring and summer and for Arabian Sea stations in the intermonsoon period (Angel and Baker, 1982; Koppelman and Weikert, 1997). RMT1 samples at more southerly stations (Gulf of Aden and Somali Coast) yield values of 7–43 ml (= g) m⁻² (extrapolated from the top 100 m; Schalk and Van Couwelaar, in Baars, 1994).

The day micronekton (RMT8) biomass level, integrated over 900 m, of 15.9 ml m⁻², is somewhat lower than those of the two temperate Atlantic stations (24.0 and 20.9 ml m⁻²) but similar to that of a subtropical one at 20° N (13.1 ml m⁻²) (Angel and Baker, 1982). It exceeds those of five stations close to the Azores (5.4–14.4 ml

m^{-2} ; Angel, 1989). The most comprehensive data set for the North West Indian Ocean is that of the Netherlands programme of 1992–1993 (Schalk and Van Couwelaar, in Baars, 1994; Van Couwelaar, 1997) which also employed RMT1 and RMT8 nets. Their stations range from 6°N to 13°N , spanning the southern limits of the most severe oxygen minimum layer. Their RMT8 biomass values from all sampling horizons between the surface and 1000 m range from $0.003\text{--}0.045 \text{ ml m}^{-3}$, while ours range from $0.0004\text{--}0.045 \text{ ml m}^{-3}$. Their six stations which were sampled to 1000 m give integrated standing stocks of micronekton ranging from $8\text{--}19 \text{ ml m}^{-2}$ by day and $11\text{--}27 \text{ ml m}^{-2}$ by night, compared with our $0\text{--}1000 \text{ m}$ values of 17.3 ml m^{-2} by day and 7.4 ml m^{-2} by night (Herring and Hargreaves, 1998). Clearly the overall standing stock is not very different, though its vertical distribution is. They found low values near the surface during the day, but the $0\text{--}100 \text{ m}$ horizon often had the highest biomass at night. The populations at their stations spread more evenly throughout the water column by day, probably responding to less severe oxygen levels at mesopelagic depths.

The increase in the biomass of micronekton in the top 100 m at night at all stations is mainly the result of diel vertical migration; at our stations this means from within the low oxygen layer. Even by day the biomass below the oxycline is very low, but at night, as indicated both by the RMT samples and the ADCP data, it becomes minimal. The daytime biomass peaks in the $200\text{--}400 \text{ m}$ depth range are largely caused by two or three species of myctophid and photichthyid fishes. The increase in the relative importance of decapods and coelenterates at the same depths at night reflects the movement of these fishes away from them to the surface. These migrations are vividly emphasised by the ADCP data which identify the extreme paucity of the biological backscatter below the oxycline at night. In the nearby Gulf of Oman the densities of myctophid fishes below the oxycline by day may reach $5\text{--}10 \text{ m}^{-3}$ (Gjosaeter, 1981). We never caught as many fish at night near the surface as we did deeper by day. This is a reversal of the usual pattern in oceanic waters and was noticed previously by Kinzer et al. (1993) using open midwater trawls. These authors speculated that this apparent reduction in daytime net avoidance might be related to increased lethargy in the low oxygen environment. We have subsequently (February 1997) encountered similar differences in the day/night catch rate of midwater fishes during a cruise in the Gulf of Oman. The RMT system, however, tends to undersample the top 10 m of the water column and this could contribute to the disparity.

Our CTD data show that the oxygen minimum layer impinges on the shelf, and the unusually low biomass below 100 m at the shelf station perhaps reflects this feature (cf. Judkins, 1980). The slope and shelf stations are spatially close yet the midwater fishes on the slope do not extend on to the shelf, even at night. This suggests that the species are unable to adapt their vertical distributions and agrees with the finding in the North Atlantic Ocean that the horizontal distribution of oceanic mesopelagic species is usually truncated by the continental slope (Merrett, 1986). Close to the lower limit of the oxygen minimum layer (ca 1100 m) there is some suggestion of a slight increase in RMT8 biomass (in contrast to the expected logarithmic decrease with depth; Angel and Baker, 1982) and the appearance of a

more typical and diverse bathypelagic fauna, compared with the depauperate mesopelagic fauna above. A zooplankton abundance peak at the lower interface of the oxygen minimum zone (740–800 m) near a seamount in the Eastern Tropical Pacific Ocean has been reported (Wishner, 1991; Wishner et al., 1995; Saltzman and Wishner, 1997a, b) using a MOCNESS system with a mesh size (335 μm) similar to that of the RMT1 (330 μm). A similar enhancement in the Arabian Sea was identified by Koppelman and Weikert (1997) but our RMT1 data are too limited to demonstrate any increase in biomass for this size range of organisms in our study area (the higher value in the daytime 900–1000 m sample was caused by a single large medusa).

For those species living all or part of their lives within the oxygen minimum layer some respiratory adaptations are likely. Increases in gill size and/or number have been described in certain fishes (e.g. endemic species of *Scopelarchus*, *Chauliodus* and *Astronesthes*; Wessel and Johnson, 1996). Some of the decapod shrimp species characteristic of our midwater samples appear to have similar adaptations, and there are likely to be additional physiological features adapting the fauna to this environment (Childress, 1975).

The oxygen minimum zone, maintained in part by the high seasonal production at the surface, puts considerable limits on the exploitation of that production by the zooplankton and micronekton. Those few species that can adapt to the extreme conditions (e.g. some decapods and fishes) are very abundant, but many species of the mesopelagic fauna of the equatorial Indian Ocean that might otherwise have been expected to be present are missing from the region. If there are smaller populations of migrants within the oxygen minimum layer than in other areas (and there are insufficient data to confirm this) the resulting reduction in the near-surface predation pressure at night may also contribute to the high zooplankton abundances near the surface. Swarms and patches of rapidly reproducing gelatinous animals may be even more readily generated under these conditions than is normally the case (Legovic, 1987). The spatial and temporal patchiness of the surface conditions may also select for the smaller zooplankton (e.g. the cyclopoid and poecilostomatoid copepods targeted by myctophids; Kinzer et al., 1993) whose short generation times give them an advantage in the exploitation of the locally ephemeral conditions. These species were numerically dominant in the area in both monsoons in a survey carried out in 1979 (Smith, 1982). Rapid growth rates and short generation times in both the much larger copepod *Calanoides carinatus* and the myctophid fishes have been suggested by S. L. Smith (1995) as key features in their monsoon-based cyclical dominance in the region, corresponding to the huge increase in diatom populations generated by the upwelling. Small size may also be of advantage to those micronekton (including the myctophids) that can live within the oxygen minimum, in that the ratio of gill area to body volume will be high, regardless of any additional relative increase in gill size. Wishner et al. (1995) identified an increase in zooplankton size from those within the oxygen minimum to those at its lower interface in the Eastern Tropical Pacific. Nevertheless it will require more detailed sampling of the mesopelagic fauna of regions with persistent oxygen minimum layers, and comparison with

equivalent faunas elsewhere, to establish whether this is a general feature of these environments.

5. Acknowledgements

We are most grateful to the Master and crew of RRS Discovery for their support throughout the cruise. Technical assistance with sampling and analysis was expertly provided on board by Daniel Ballesterio, Rebecca Bellerby, Martin Beney, Ben Boorman, Dave Edge, Jeff Jones, Steve Keene, Alex Megann, Ben Moat, Bob Wallace and Simon Watts, and ashore by Sophie Fielding and Pat Hargreaves. The suggestions of two anonymous referees greatly improved the revised text.

6. References

- Allredge, A.L., Robison, B.H., Fleminger, A., Torres, J.J., King, J.M., & Hamner, W.M. (1984). Direct sampling and in situ observation of a persistent copepod aggregation in the mesopelagic zone of the Santa Barbara Basin. *Marine Biology*, 80, 75–81.
- Allen, J.T., Smeed, D.A., & Chadwick, A.L. (1994). Eddies and mixing at the Iceland-Faeroes front. *Deep-Sea Research* 1, 41, 51–79.
- Angel, M.V., & Baker, A.C. (1982). Vertical distribution of standing crop of plankton and micronekton at three stations in the northeast Atlantic. *Biological Oceanography*, 2, 1–30.
- Angel, M.V. (1989). Vertical profiles of pelagic communities in the vicinity of the Azores Front and their implications to deep ocean ecology. *Progress in Oceanography*, 22, 1–46.
- Baars, M. A. (Ed.). (1994). Monsoons and pelagic ecosystems, vol. 1. National Museum of Natural History, Leiden, Netherlands.
- Banse, K. (1994). On the coupling of hydrography, phytoplankton, zooplankton and settling particles offshore in the Arabian Sea. In D. Lal (Ed.), *Biogeochemistry of the Arabian Sea*. Indian Academy of Sciences, pp. 27–63.
- Bruce, J.G. (1974). Some details of upwelling off the Somali and Arabian coasts. *Journal of Marine Research*, 32, 419–432.
- Bauer, S., Hitchcock, G.L., & Olson, D.B. (1991). Influence of monsoonally-forced Ekman dynamics upon surface layer depth and plankton biomass distribution in the Arabian Sea. *Deep-Sea Research*, 38, 531–553.
- Childress, J.J. (1975). The respiratory rates of midwater crustaceans as a function of depth of occurrence and relation to the oxygen minimum layer off Southern California. *Comparative Biochemistry and Physiology*, 50A, 787–799.
- Cohen, D. M. (1973). Zoogeography of the fishes of the Indian Ocean. In B. Zeitschel, & S. A. Gerlach (Eds.), *The Biology of the Indian Ocean*. Springer Verlag, pp. 451–463.
- Currie, R.I. (1992). Circulation and upwelling off the coast of South-East Arabia. *Oceanologica Acta*, 15, 43–60.
- Dalpadado, P., & Gjosaeter, J. (1988). Feeding ecology of the lanternfish *Benthosema pterotum* from the Indian Ocean. *Marine Biology*, 99, 555–567.
- Elliott, A.J., & Savidge, G. (1990). Some features of the upwelling off Oman. *Journal of Marine Research*, 48, 319–333.
- Flagg, C.N., & Smith, S.L. (1989). On the use of the Acoustic Doppler Current Profiler to measure zooplankton abundance. *Deep-Sea Research*, 36, 455–474.
- Francois, R.E., & Garrison, G.R. (1982). Sound absorption based on ocean measurements. Part II: Boric acid contribution and equations for total absorption. *Journal of the Acoustic Society of America*, 72, 1879–1890.

- Gjosæter, J. (1981). Abundance and production of lanternfish (Myctophidae) in the western and northern Arabian Sea. *Fiskeridirektoratets Skrifter Serie Havundersøkelser*, 17, 215–251.
- Gjosæter, J. (1984). Mesopelagic fish, a large potential resource in the Arabian Sea. *Deep-Sea Research*, 31, 1019–1035.
- GLOBEC. (1993). Implementation plan and workshop report for US GLOBEC studies in the Arabian Sea. US GLOBEC Report. U.S.GLOBEC Division of Environmental Studies, University of California, Davis, California. No. 9, 105 pp.
- Griffiths, G., & Diaz, J.I. (1996). Comparison of acoustic backscatter measurements from a ship-mounted Acoustic Doppler Current Profiler and an EKB500 scientific echosounder. *ICES Journal of Marine Science*, 53, 487–491.
- Herring, P. J., & Hargreaves, P. M. (1998). The vertical distribution of biomass in the Arabian Sea near Oman (19° N, 59° E) during the southwest monsoon, and its relation to the oxygen minimum. *Proceedings of the 2nd International Congress on Pelagic Biogeography*. IOC/UNESCO Workshop report no. 142.
- Hubold, G., Hempel, I., & Meyer, M. (1988). Zooplankton communities in the southern Weddell Sea (Antarctica). *Polar Biology*, 8, 225–233.
- Ignat'ev, S.M. (1995). Soviet research on zooplankton in the Arabian Sea. *Russian Journal of Marine Biology*, 21, 77–79.
- Ikeda, T. (1974). Nutritional ecology of zooplankton. *Memoirs of the Faculty of Fisheries, Hokkaido University*, 22, 1–97.
- Judkins, D.C. (1980). Vertical distribution of zooplankton in relation to the oxygen minimum off Peru. *Deep-Sea Research*, 27, 475–487.
- Kindle, J., Young, D. K., Arnone, R. A., & Green, D. W. (1996). Biophysical interactions in the Arabian Sea. *NRL Review* 149–151.
- Kinzer, J., Botterger-Schnack, R., & Scholz, K. (1993). Aspects of horizontal distribution and diet of myctophid fish in the Arabian Sea with reference to the deep water oxygen deficiency. *Deep-Sea Research*, 40, 783–800.
- Koppelman, R., & Weikert, H. (1997). Deep Arabian Sea mesozooplankton distribution. Intermonsoon, October 1995. *Marine Biology*, 129, 549–560.
- Larson, R.J. (1986). Water content, organic content, and carbon and nitrogen composition of medusae from the Northeast Pacific. *Journal of Experimental Marine Biology and Ecology*, 99, 107–120.
- Larson, R.J. (1987). A note on the feeding, growth, and reproduction of the epipelagic scyphomedusa *Pelagia noctiluca* (Forsk.). *Biological Oceanography*, 4, 447–454.
- Lefevre, J. (1986). Aspects of the biology of frontal systems. *Advances in Marine Biology*, 23, 163–299.
- Legovic, T. (1987). A recent increase in jellyfish populations: a predator-prey model and its implications. *Ecological Modelling*, 38, 243–256.
- Longhurst, A.R. (1967). Vertical distribution of zooplankton in relation to the eastern Pacific oxygen minimum. *Deep-Sea Research*, 14, 51–63.
- Madhupratap, M., Nair, S.R.S., Haridas, P., & Padmavati, G. (1990). Response of zooplankton to physical changes in the environment: coastal upwelling along central west coast of India. *Journal of Coastal Research*, 6, 413–426.
- Malej, A. (1989). Behaviour and trophic ecology of the jellyfish *Pelagia noctiluca* (Forsskal). *Journal of Experimental Marine Biology and Ecology*, 126, 259–270.
- Mantoura, R. F. C. (1995). Arabesque I: cruise report. Plymouth Marine Laboratory, Plymouth PL1 3DH, U.K., 102 pp.
- Merrett, N.R. (1986). Biogeography of the oceanic rim: a poorly known zone of ichthyofaunal interaction. *UNESCO Technical Papers in Marine Science*, 49, 201–209.
- Olson, D.B., Hitchcock, G.B., Fine, R.A., & Warren, B.A. (1993). Maintenance of the low-oxygen layer in the central Arabian Sea. *Deep-Sea Research*, 40, 673–685.
- Packard, T. T., Garfield, P. C., & Codispoti, L. A. (1983). Oxygen consumption and denitrification below the Peruvian upwelling. In E. Suess, & J. Thiede (Eds.), *Coastal upwelling: its sediment record. Part A: Responses of the sedimentary regime to present coastal upwelling*. Plenum Press, New York., pp. 147–173.

- Plueddemann, A.J., & Pinkel, R. (1989). Characterisation of the patterns of diel vertical migration using a Doppler Sonar. *Deep-Sea Research*, 36, 509–530.
- Premchad, K., Sastry, J.S., & Murty, C.S. (1986). Watermass structure in the Western Indian Ocean B Part II: the spreading and transformation of the Persian Gulf Water. *Mausam*, 37, 179–186.
- Pugh, P.R., Pages, F., & Boorman, B. (1997). The vertical distribution and abundance of pelagic cnidarians in the eastern Weddell Sea, Antarctica. *Journal of the Marine Biological Association of the United Kingdom*, 77, 341–360.
- Qasim, S.Z. (1982). Oceanography of the northern Arabian Sea. *Deep-Sea Research*, 29, 1041–1068.
- Roe, H.S.J., & Shale, D.M. (1979). A new multiple rectangular midwater trawl (RMT1 + 8M) and some modifications to the Institute of Oceanographic Sciences' RMT1 + 8. *Marine Biology*, 50, 283–288.
- Roe, H.S.J., Baker, A.D.E.C., Carson, R.M., Wild, R.A., & Shale, D.M. (1980). Behaviour of the Institute of Oceanographic Sciences' Rectangular Midwater Trawls; theoretical aspects and experimental observations. *Marine Biology*, 56, 247–259.
- Roe, H. S. J., Hartman, M. C., Crisp, N. A., & Griffiths, G. (1995). Bioacoustic variability in the North Atlantic and Northwest Indian Oceans. Contract final report for the Defence Research Agency, 85 pp. ISBN 0–904175–24–3.
- Roe, H.S.J., Griffiths, G., Hartman, M.C., & Crisp, N.A. (1996). Variability in biological distributions and hydrography from concurrent Acoustic Doppler Current profiler and SeaSoar surveys. *ICES Journal of Marine Science*, 53, 131–138.
- Ropke, W., Nellen, W., & Piatkowski, U. (1993). A comparative study on the influence of the pycnocline on the vertical distribution of fish larvae and cephalopod paralarvae in three ecologically different areas of the Arabian Sea. *Deep-Sea Research*, 40, 801–819.
- Shetye, S. R., Gouveia, A. D., & Shenoi, S. S. C. (1994). Circulation and water masses of the Arabian Sea. In D. Lal (Ed.), *Biogeochemistry of the Arabian Sea*. Indian Academy of Sciences, pp. 9–25.
- Saltzman, J., & Wishner, K.F. (1997). Zooplankton ecology in the eastern tropical Pacific oxygen minimum zone above a seamount: 1 General trends. *Deep-Sea Research*, 44, 907–930.
- Saltzman, J., & Wishner, K.F. (1997). Zooplankton ecology in the eastern tropical Pacific oxygen minimum zone above a seamount: 2 Vertical distribution of copepods. *Deep-Sea Research*, 44, 931–954.
- Smith, S.L. (1995). The Arabian Sea: mesozooplankton response to seasonal climate in a tropical ocean. *ICES Journal of Marine Science*, 52, 427–438.
- Smith, R. L. (1995). The physical processes of coastal upwelling systems. In C. P. Summerhayes, K.-C. Emeis, M. V. Angel, R. L. Smith, & B. Zeitschel (Eds.), *upwelling in the oceans: modern processes and ancient records*. John Wiley and Sons, Chichester, pp. 39–64.
- Smith, R. L., & Bottero, J. S. (1977). On upwelling in the Arabian Sea. In M. V. Angel (Ed.), *A voyage of Discovery*. Pergamon Press, pp. 291–304.
- Smith, S. L., Banse, K., Cochran, J. K., Codispoti, L. A., Ducklow, H. W., Luther, M. E., Olson, D. B., Peterson, W. T., Prell, W. L., Surgi, N., Swallow, J. C., & Wishner, K. (Eds.). (1991). U.S.JGOFS: Arabian Sea Process Study, U.S.JGOFS Planning Report No.13. Woods Hole Oceanographic Institution, Woods Hole, MA, 164 pp.
- Smith, S.L. (1982). The northwest Indian Ocean during the monsoons of 1979: distribution, abundance and feeding of zooplankton. *Deep-Sea Research*, 29, 1331–1353.
- Smith, S.L. (1984). Biological indications of active upwelling in the northwestern Indian Ocean in 1964 and 1979, and a comparison with Peru and northwest Africa. *Deep-Sea Research*, 31, 951–967.
- Swallow, J.C. (1984). Some aspects of the physical oceanography of the Indian Ocean. *Deep-Sea Research*, 31, 639–650.
- Theberge, S.M., Luther, G.W., & Farrenkopf, A.M. (1997). On the existence of free and metal complexed sulfide in the Arabian Sea and its oxygen minimum. *Deep-Sea Research II*, 44, 1381–1390.
- Van Couwelaar, M. (1997). Zooplankton and micronekton biomass off Somalia and in the southern Red Sea during the SW monsoon of 1992 and the NE monsoon of 1993. *Deep-Sea Research II*, 44, 1213–1234.
- Van Couwelaar, M., Angel, M.V., & Madin, L.P. (1997). The distribution and biology of the swimming crab *Charybdis smithii* McLeay, 1838 (Crustacea; Brachyura; Portunidae) in the NW Indian Ocean. *Deep-Sea Research II*, 44, 1251–1280.

- Vinogradov, M.E., & Voronina, N.M. (1962). Influence of the oxygen deficit on the distribution of plankton in the Arabian Sea. *Deep-Sea Research*, 9, 523–530.
- Vinogradov, M. E. (1970). Vertical distribution of the oceanic zooplankton. Israel Program for Scientific Translations, Jerusalem, 339 pp.
- Warren, B. A. (1994). Context of the suboxic layer in the Arabian Sea. In D. Lal (Ed.), *Biogeochemistry of the Arabian Sea*. Indian Academy of Sciences, pp. 203–216.
- Weeks, A.R., Griffiths, G., Roe, H.S.J., Moore, G., Robinson, I.S., Atkinson, A., & Shreeve, R. (1995). The distribution of acoustic backscatter from zooplankton compared with the physical structure, phytoplankton and radiance distribution during the spring bloom in the Bellingshausen Sea. *Deep-Sea Research*, 42, 97–1019.
- Weeks, A. R., Ballesterio, D., & Robinson, I. S. (1997). Optical properties of the upper ocean in the Arabian Sea in August 1994. *Ocean Optics XIII*, vol. 2963. Society of Photo-optical Engineers, pp. 570–578.
- Wessel, J. H., & Johnson, R. K. (1996). Commonality and uniqueness in the biogeography of Indian Ocean mesopelagic fishes. In M. F. Thompson, & N. M. Tirmizi (Eds.), *The Arabian Sea: living marine resources and the environment*. Balkema, pp. 295–308.
- Wiebe, P.W. (1988). Functional regression equations for zooplankton displacement volume, wet weight, dry weight, and carbon: a correction. *Fishery Bulletin*, 86, 833–835.
- Wishner, K. F. (1991). Oxygen minimum zone interfaces. In S. L. Smith, K. Banse, J. K. Cochran, L. A. Codispoti, H. W. Ducklow, M. E. Luther, D. B. Olson, W. T. Peterson, W. L. Prell, N. Surgi, J. C. Swallow, & K. Wishner (Eds.), *U.S.JGOFS Arabian Sea Process Study*. U.S.JGOFS Planning Report No. 13. Woods Hole Oceanographic Institution, Woods Hole, MA, p. 107.
- Wishner, K.F., Ashjian, C.J., Gelfman, C., Gowing, M., Levin, L.A., Mullineaux, L.S., & Saltzman, J. (1995). Pelagic and benthic ecology of the lower interface of the Eastern Tropical Pacific oxygen minimum layer. *Deep-Sea Research*, 42, 93–115.
- WOCE. (1992). Indian Ocean Special Studies 2.ISS-2., Report of WOCE Working Group, Chairman D.B. Olson. 20 pp. (unpublished report)
- WOCE. (1993). US contribution to WOCE Core Project 1. The program design for the Indian Ocean. US WOCE Office, February 1993, 80 pp.
- Wyrtki, K. (1971). Oceanographic Atlas of the International Indian Ocean Expedition. National Science Foundation, US Government Printing Office, 531 pp.
- Wyrtki, K. (1973). Physical oceanography of the Indian Ocean. In B. Zeitschel, & S. A. Gerlach (Eds.), *The biology of the Indian Ocean*. Springer-Verlag, pp. 18–36.
- Zeitschel, B., & Gerlach, S. A. (Eds.). (1973). *The biology of the Indian Ocean*. Springer Verlag, Berlin, 549 pp.